

1 Dear editor,

2 Thank you very much for your efforts in the review process. We are happy to receive such good news!

3 We have made some minor changes according to the manuscript preparation requests of GMD, such  
4 as: Changing “Figure” to “Fig.”, changing “Section” to “Sect.”, embedding fonts into the figures,  
5 changed the table design to only have horizontal lines, double-checked the references and other minor  
6 changes. Lastly we added to units to the RMSE in the abstract as requested.

7 We hope these details (and attached manuscript mark-up) sufficiently describes the manuscript changes  
8 made. We are looking forward to the proof version of our manuscript.

9 Sincerely,

10 Bram Droppers on behalf of all co-authors

1 **Simulating human impacts on global water resources using**  
2 **VIC-5**

3 Bram Droppers<sup>1</sup>, Wietse H.P. Franssen<sup>1</sup>, Michelle T.H. van Vliet<sup>2</sup>, Bart Nijssen<sup>3</sup>, Fulco  
4 Ludwig<sup>1</sup>

5 <sup>1</sup> Water Systems and Global Change Group, Department of Environmental Sciences, Wageningen  
6 University, Wageningen, 6708 PB, The Netherlands

7 <sup>2</sup> Department of Physical Geography, Utrecht University, Utrecht, 3584 CS, The Netherlands

8 <sup>3</sup> Computational Hydrology Group, Department of Civil and Environmental Engineering, University of  
9 Washington, Seattle, 98195, United States of America

10 *Correspondence to:* Bram Droppers (bram.droppers@wur.nl)

11 **Abstract.** Questions related to historical and future water resources and scarcity have been addressed  
12 by several macro-scale hydrological models. One of these models is the Variable Infiltration Capacity  
13 (VIC) model. However, further model developments were needed to holistically assess anthropogenic  
14 impacts on global water resources using VIC.

15 Our study developed VIC-WUR, which extends the VIC model with: (1) integrated routing, (2) surface  
16 and groundwater use for various sectors (irrigation, domestic, industrial, energy, and livestock), (3)  
17 environmental flow requirements for both surface and groundwater systems, and (4) dam operation.  
18 Global gridded datasets on sectoral demands were developed separately and used as an input to the VIC-  
19 WUR model.

20 Simulated national water withdrawals were in line with reported FAO national annual withdrawals ( $R^2$   
21 adjusted  $R^2 > 0.8$ ), both per sector as well as per source. However, trends in time for domestic and  
22 industrial water withdrawal were mixed compared to other previous studies. GRACE monthly terrestrial  
23 water storage anomalies were well represented (global mean RMSE of 1.9 mm and 3.5 mm for annual  
24 and interannual anomalies respectively), while groundwater depletion trends were overestimated. The  
25 implemented human impact modules increased simulated streamflow performance for 370 out of 462  
26 human-impacted GRDC monitoring stations, mostly due to the effects of reservoir operation. An  
27 assessment of environmental flow requirements indicates that global water withdrawals have to be  
28 severely limited (by 39 %) to protect aquatic ecosystems, especially for groundwater withdrawals.

29 VIC-WUR has potential for studying impacts of climate change and anthropogenic developments on  
30 current and future water resources and sectoral specific-water scarcity. The additions presented here  
31 make the VIC model more suited for fully-integrated worldwide water-resource assessments.

## 32 1 Introduction

33 Questions related to historical and future water resources and scarcity have been addressed by several  
34 macro-scale hydrological models over the last few decades (Liang et al., 1994; Alcamo et al., 1997;  
35 Hagemann and Gates, 2001; Takata et al., 2003; Krinner et al., 2005; Bondeau et al., 2007; Hanasaki et  
36 al., 2008b; ~~Vanyan~~ Beek and Bierkens, ~~2008~~2009; Best et al., 2011). Early efforts focussed on the  
37 simulation of natural water resources and the impacts of land cover and climate change on water  
38 availability (Oki et al., 1995; Nijssen et al., 2001a; Nijssen et al., 2001b). Recently, a larger focus has  
39 been on incorporating anthropogenic impacts, such as water withdrawals and dam operations, into water  
40 resource assessments (Alcamo et al., 2003; Haddeland et al., 2006b; Biemans et al., 2011; Wada et al.,  
41 2011b; Hanasaki et al., 2018).

42 Global water withdrawals increased eight-fold over the last century and are projected to increase further  
43 (Shiklomanov, 2000; Wada et al., 2011a). Although water withdrawals are only a small fraction of the  
44 total global runoff (Oki and Kanae, 2006), water scarcity can be severe due to the variability of water in  
45 both time and space (Postel et al., 1996). Already severe water scarcity is experienced by two-thirds of  
46 the global population for at least part of the year (Mekonnen and Hoekstra, 2016). To stabilize water  
47 availability for different sectors (e.g. irrigation, hydropower, and domestic uses) dams and reservoirs  
48 were built, which are able to strongly affect global river streamflow (Nilsson et al., 2005; Grill et al.,  
49 2019). In addition, groundwater resources are being extensively exploited to meet increasing water  
50 demands (Rodell et al., 2009; Famiglietti, 2014).

51 One of widely-used macro-scale hydrological models is the Variable Infiltration Capacity (VIC) model.  
52 The model was originally developed as a land-surface model (Liang et al., 1994), but has been mostly  
53 used as a stand-alone hydrological model (Abdulla et al., 1996; Nijssen et al., 1997) using an offline  
54 routing module (Lohmann et al., 1996; Lohmann et al., ~~1998a, b~~1998b, a). Where land-surface models  
55 focus on the vertical exchange of water and energy between the land surface and the atmosphere,  
56 hydrological models focus on the lateral movement and availability of water. By combining these two  
57 approaches, VIC simulations are strongly process-based and this, in turn, provides a good basis for  
58 climate-impact modelling.

59 VIC has been used extensively in studies ranging from: coupled regional climate model simulations  
60 (Zhu et al., 2009; Hamman et al., 2016), combined river streamflow and water-temperature simulations  
61 (van Vliet et al., 2016), hydrological sensitivity to climate change (Hamlet and Lettenmaier, 1999;  
62 Nijssen et al., 2001a; Chegwidden et al., 2019), global streamflow simulations (Nijssen et al., 2001b),  
63 sensitivity in flow regulation and redistribution (Voisin et al., 2018; Zhou et al., 2018), and real-time  
64 drought forecasting (Wood and Lettenmaier, 2006; Mo, 2008). Several studies used VIC to simulate the  
65 anthropogenic impacts of irrigation and dam operation on water resources (Haddeland et al., 2006a;  
66 Haddeland et al., 2006b; Zhou et al., 2015; Zhou et al., 2016) based on the model setup of Haddeland et  
67 al. (2006b). However, further developments were needed to holistically assess anthropogenic impacts  
68 on global water resources using VIC (Nazemi and Wheatler, 2015a, b; Döll et al., 2016; Pokhrel et al.,  
69 2016).

70 Firstly, the VIC model did not yet include groundwater withdrawals or water withdrawals from  
71 domestic, manufacturing, and energy (thermoelectric) sources. Although these sectors use less water  
72 than irrigation (Shiklomanov, 2000; Grobicki et al., 2005; Hejazi et al., 2014) they are locally important  
73 actors (Gleick et al., 2013)(Gleick et al., 2013), especially for the water-food-energy nexus (Bazilian et  
74 al., 2011). Sufficient water supply and availability are essential for meeting a range of local and global  
75 sustainable development goals related to water, food, energy, and ecosystems (Bijl et al., 2018).  
76 Secondly, environmental flow requirements (EFRs) were often neglected (Pastor et al., 2014), even  
77 though they are “necessary to sustain aquatic ecosystems which, in turn, support human cultures,  
78 economies, sustainable livelihoods, and well-being” (Brisbane Declaration, 2017). Anthropogenic  
79 alterations already strongly affect freshwater ecosystems (Carpenter et al., 2011), with more than a  
80 quarter of all global rivers experiencing very high biodiversity threats (Vorosmarty et al., 2010). By  
81 neglecting EFRs, sustainable water availability for anthropogenic uses is overestimated (Gerten et al.,  
82 2013). Lastly, while the model setup of Haddeland et al. (2006b) already included important  
83 anthropogenic impact modules (i.e. irrigation and dam operation), these were not fully integrated yet.  
84 Therefore multiple successive model runs were required (see [Section Sect. 2.1](#)) which was  
85 computationally expensive, especially for global water resources assessments.

86 Recently version 5 of the VIC model (VIC-5) was released (Hamman et al., 2018), which focussed on  
87 improving the VIC model infrastructure. These improvements provide the opportunity to fully integrate  
88 human-impacts into the VIC model framework, while reducing computation times. Here the newly  
89 developed VIC-WUR model is presented (named after the developing team at Wageningen University  
90 and Research). The VIC-WUR model extends the existing VIC-5 model with several modules that  
91 simulate the anthropogenic impacts on water resources. These modules will implement previous major  
92 works on anthropogenic impact modelling as well as integrate environmental flow requirements into  
93 VIC-5. The modules include: (1) integrated routing, (2) surface and groundwater use for various sectors  
94 (irrigation, domestic, industrial, energy and livestock), (3) environmental flow requirements for both  
95 surface and groundwater systems, and (4) dam operation.

96 The next section first describes the original VIC-5 hydrological model (~~Section~~Sect. 2.1), which  
97 calculates natural water resource availability. Subsequently the integration of the anthropogenic impact  
98 modules, which modify the water resource availability, are described (~~Section~~Sect. 2.2). Global  
99 anthropogenic water uses for each sector are also estimated (~~Section~~Sect. 2.3). To assess the capability  
100 of the newly developed modules, the VIC-WUR results were compared with FAO national water  
101 withdrawals by sector and by source (~~FAO, 2016~~(FAO, 2016); Huang et al. (2018), ~~Steinfeld et al.~~  
102 ~~(2006)~~Steinfeld et al. (2006), and Shiklomanov (2000) data on water withdrawals by sector; GRACE  
103 terrestrial water storage anomalies (~~NASA, 2002~~(NASA, 2002); GRDC streamflow timeseries (~~GRDC,~~  
104 ~~2003~~(GRDC, 2003)); and Yassin et al. (2019) and Hanasaki et al. (2006) data on reservoir operation  
105 (~~Section~~Sect. 3.2). VIC-WUR simulations results are also compared with various other state-of-the-art  
106 global hydrological models. Lastly, the impacts of adhering to surface and groundwater environmental  
107 flow requirements on water availability are assessed (~~Section~~Sect. 3.3). This assessment is included to  
108 indicate the effects of the newly integrated surface and groundwater environmental flow requirements  
109 on worldwide water availability.

## 110 2 Model development

### 111 2.1 VIC hydrological model

112 The basis of the VIC-WUR model is the Variable Infiltration Capacity model version 5 (VIC-5) (Liang  
113 et al., 1994; Hamman et al., 2018). VIC-5 is an open source macro-scale hydrological model that  
114 simulates the full water and energy balance on a (latitude – longitude) grid. Each grid cell accounts for  
115 sub-grid variability in land cover and topography, and allows for variable saturation across the grid cell.  
116 For each sub-grid the water and energy balance is computed individually (i.e. sub-grid do not exchange  
117 water or energy between one another). The methods used to calculate the water and energy balance are  
118 summarized in Appendix A, mainly based on the work of Liang et al. (1994). For the description of the  
119 global calibration and validation of the water balance one is referred to Nijssen et al. (2001b).

120 VIC version 5 (Hamman et al., 2018) upgrades did not change the model representation of physical  
121 processes, but improved the model infrastructure. Improvements include the use of NetCDF for  
122 input/output and the implementation of parallelization through Message Passing Interface (MPI). These  
123 changes increase computational speed and make VIC-5 better suited for (computationally expensive)  
124 global simulations. The most significant modification that enables new model applications is that VIC-  
125 5 also changed the processing order of the model. In previous versions all timesteps were processed for  
126 a single grid cell before continuing to the next cell (time-before-space). In VIC-5 all grid cells are  
127 processed before continuing to the next timestep (space-before-time). This development allows for  
128 interaction between grid cells every timestep, which is important for full integration of the anthropogenic  
129 impact modules, especially water withdrawals and dam operation.

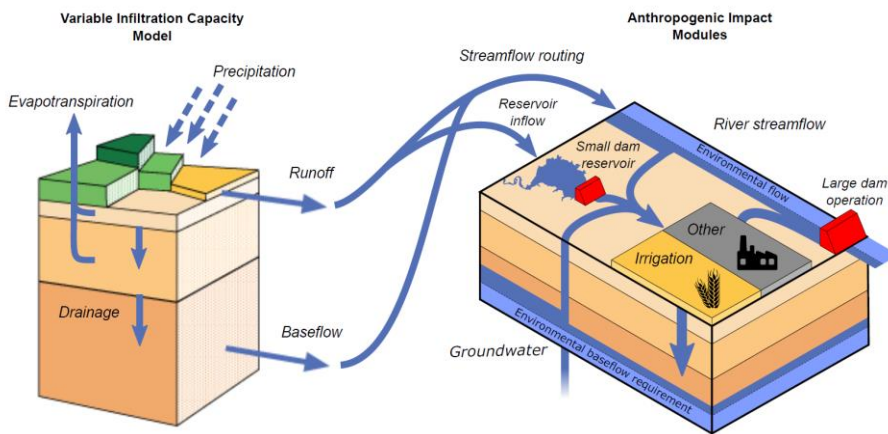
130 For example, surface and subsurface runoff routing to produce river streamflow was typically done as a  
131 post-process operation (Lohmann et al., 1996; Hamman et al., 2017), due to the time-before-space  
132 processing order of previous versions. In order for reservoirs to account for downstream water demand,  
133 an irrigation demand initialization was required. This initialization could either be an independent offline  
134 dataset (~~Voisin et al., 2013a~~)(Voisin et al., 2013a) or multiple successive model runs (Haddeland et al.,  
135 2006b). Since VIC-5 uses the space-before-time processing order, irrigation water demands and runoff  
136 routing could be simulated each timestep. The routing post-process was replaced by our newly

137 developed routing module, which simulates routing sequentially (upstream-to-downstream) based on  
138 the Lohmann et al. (1996) equations.

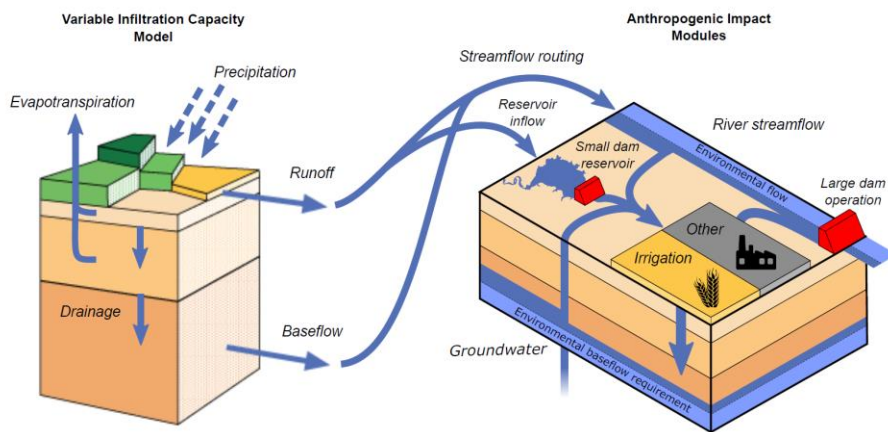
## 139 2.2 Anthropogenic-impact modules

140 VIC-WUR extends the existing VIC-5 though the addition of several newly implemented  
141 anthropogenic-impact modules (Figure Fig. 1). These modules include sector-specific water withdrawal  
142 and consumption, environmental flow requirements for both surface and groundwater systems, and dam  
143 operation for large and small (within-grid) dams.

144



145





146 Figure 1: Schematic overview of the VIC-WUR model that includes the VIC-5 model (left) and several anthropogenic  
147 impact modules. (right). Water from river streamflow, groundwater, and small (within-grid) reservoirs are available  
148 for withdrawal. Surface and groundwater withdrawals are constrained by environmental flow requirements.  
149 Withdrawn water is available for irrigation, domestic, industrial, energy, and livestock use. Unconsumed irrigation  
150 water is returned to the soil column of the hydrological model. Unconsumed water for the other sectors is returned to  
151 the river streamflow. Small reservoirs fill using surface runoff from the cell they are located, while large dam reservoirs  
152 operate solely on rivers streamflow.

### 153 2.2.1 Water withdrawal and consumption

154 In VIC-WUR, sectoral water demands need to be specified for each grid cell (Section 2.3). To meet  
155 water demands, water can be withdrawn from river streamflow, small (within-grid) reservoirs, and  
156 groundwater resources. Streamflow withdrawals are abstracted from the grid cell discharge (as  
157 generated by the routing module) and reservoir withdrawals are abstracted from small dam reservoirs  
158 (located in the cell). Groundwater withdrawals are abstracted from the third layer soil moisture and an  
159 (unlimited) aquifer below the soil column. Aquifer abstractions represent renewable and non-renewable  
160 abstractions from deep groundwater resources. Subsurface runoff is used to fill the aquifer if there is a  
161 deficit.

162 The partitioning of water withdrawals between surface and ground water resources is data driven  
163 (similar to e.g. Döll et al., 2012; Voisin et al., 2017; Hanasaki et al., 2018). Partitioning was based on  
164 the study of Döll et al. (2012), who estimated groundwater withdrawal fractions for each sector in around  
165 15.000 national and sub-national administrative units. These groundwater fractions were based mainly  
166 on information from the International Groundwater Resources Assessment Centre (IGRAC; un-  
167 igrac.org) database. Surface water withdrawals were partitioned between river streamflow and small  
168 reservoirs relative to water availability. Groundwater withdrawals were first withdrawn from the third  
169 soil layer, second from the (remaining) river streamflow resources and lastly from the groundwater  
170 aquifer. This order was implemented to avoid overestimation of non-renewable groundwater  
171 withdrawals as a result of errors in the partitioning data. Aquifer withdrawals are additionally limited  
172 by the pumping capacity from Sutanudjaja et al. (2018), who estimated regional pumping capacities  
173 based on information from IGRAC.

174 Water can also be withdrawn from the river streamflow of other 'remote' cells in delta areas. Since  
175 rivers cannot split in the routing module, the model is unable to simulate the redistribution of water  
176 resources in dendritic deltas. Therefore, streamflow at the river mouth is available for use in delta areas

177 (partitioned based on demand) to simulate the actual water availability. Delta areas were delineated by  
178 the global delta map of Tessler et al. (2015).

179 In terms of water allocation, under conditions where water demands cannot be met, water withdrawals  
180 are allocated to the domestic, energy, manufacturing, livestock, and irrigation sector in that order.  
181 Withdrawn water is partly consumed, meaning the water evaporates and does not return to the  
182 hydrological model. Consumption rates were set at 0.15 for the domestic and 0.10 for the industrial  
183 sector, based on the data of Shiklomanov (2000). The water consumption in the energy sector was based  
184 on Goldstein and Smith (2002) and varies per thermoelectric plant based on the fuel type and cooling  
185 system. For the livestock sector the assumption was made that all withdrawn water is consumed.  
186 Unconsumed water withdrawals for these sectors are returned as river streamflow. For the irrigation  
187 sector, consumption was determined by the calculated evapotranspiration. Unconsumed irrigation water  
188 remains in the soil column and eventually returns as subsurface runoff.

### 189 **2.2.2 Environmental flow requirements**

190 Water withdrawals can be constrained by environmental flow requirements (EFRs). These EFRs specify  
191 the timing and quantity of water needed to support terrestrial river ecosystems (Smakhtin et al., 2004;  
192 Pastor et al., 2019). Surface and groundwater withdrawals are constrained separately in VIC-WUR,  
193 based on the EFRs for streamflow and baseflow respectively. EFRs for streamflow specify the minimum  
194 river streamflow requirements while EFRs for baseflow specify the minimum subsurface runoff  
195 requirements (from groundwater to surface water). Since baseflow is a function groundwater  
196 availability, baseflow requirements are used to constrain groundwater (including aquifer) withdrawals.

197 Various EFR methods are available (Smakhtin et al., 2004; Richter et al., 2012; Pastor et al., 2014). Our  
198 study used the Variable Monthly Flow (VMF) method (Pastor et al., 2014) to calculate the EFRs for  
199 streamflows. VMF calculates the required streamflow as a fraction of the natural flow during high (30  
200 %), intermediate (45 %) and low (60 %) flow periods, as described in Appendix B. The VMF method  
201 performed favourably compared to other hydrological methods, in 11 case studies where EFRs were

202 calculated locally (Pastor et al., 2014). The advantage of the VMF method is that the method accounts  
203 for the natural flow variability, which is essential to support freshwater ecosystems (Poff et al., 2010).  
204 EFR methods for baseflow have been rather underdeveloped compared to EFR methods for streamflow.  
205 However, a presumptive standard of 90 % of the natural subsurface runoff through time was proposed  
206 by Gleeson and Richter (2018), as described in Appendix B. This standard should provide high levels  
207 of ecological protection, especially for groundwater dependent ecosystems.

208 Note that part of the EFRs for baseflow are already captured in the EFRs for streamflow, especially  
209 during low-flow periods that are usually dominated by baseflows. However, the EFRs for baseflow  
210 specifically limit local groundwater withdrawals while EFRs for streamflow include the accumulated  
211 runoff from upstream areas. Also, the chemical composition of groundwater derived flows is inherently  
212 different, making them a non-substitutable water flow for environmental purposes (Gleeson and Richter,  
213 2018).

### 214 **2.2.3 Dam operation**

215 Due to the lack of globally available information on local dam operations, several generic dam operation  
216 schemes were developed for macro-scale hydrological models to reproduce the effect of dams on natural  
217 streamflow (Haddeland et al., 2006a; Hanasaki et al., 2006; Zhao et al., 2016; Rougé et al., 2019; Yassin  
218 et al., 2019). In VIC-WUR a distinction is made between ‘small’ dam reservoirs (with an upstream area  
219 smaller than the cell area) and ‘large’ dam reservoirs, similar to Hanasaki et al. (2018), Wisser et al.  
220 (2010a) and Döll et al. (2009). Small dam reservoirs act as buckets that fill using surface runoff of the  
221 grid-cell they are located in and reservoirs storage can be used for water withdrawals in the same cell.  
222 Large dam reservoirs are located in the main river and used the operation scheme of Hanasaki et al.  
223 (2006), as described in Appendix C.

224 The scheme distinguishes between two dam types: (1) dams that do not account for water demands  
225 downstream (e.g. hydropower dams or flood protection dams) and (2) dams that do account for water  
226 demand downstream (e.g. irrigation dams). For dams that do not account for demands, dam release is  
227 aimed at reducing annual fluctuations in discharge. For dams that do account for demands, dam release

228 is additionally adjusted to provide more water during periods of high demand. The operation scheme  
229 was validated by Hanasaki et al. (2006) for 28 reservoirs and was used in various other studies (Hanasaki  
230 et al., 2008b; Döll et al., 2009; Pokhrel et al., 2012b; Voisin et al., 2013b; Hanasaki et al., 2018). Here,  
231 the scheme was adjusted slightly to account for monthly varying EFRs and to reduce overflow releases,  
232 which is described in Appendix C.

233 The Global Reservoir and Dam (GRanD) database (Lehner et al., 2011) was used to specify location,  
234 capacity, function (purpose), and construction year of each dam. The capacity of multiple (small- and  
235 large) dams located in the same cell were combined.

### 236 **2.3 Sectoral water demands**

237 VIC-WUR water withdrawals are based on the irrigation, domestic, industry, energy, and livestock  
238 water demand in each grid-cell. Water demands represent the potential water withdrawal, which is  
239 reduced when insufficient water is available. Irrigation demands were estimated based on the  
240 hydrological model while water demands for other sectors are provided to the model as an input.  
241 Domestic and industrial were estimated based on several socioeconomic predictors, while energy and  
242 livestock water demands were derived from power plant and livestock distribution data. Due to data  
243 limitations the energy sector was incomplete, and energy water demands were partly included in the  
244 industrial water demands (which combined the remaining energy and manufacturing water demands).  
245 For more details concerning sectoral water demand calculations the reader is referred to Appendix D.

#### 246 **2.3.1 Irrigation demands**

247 Irrigation demands were set to increase soil moisture in the root zone so that water availability is not  
248 limiting crop evapotranspiration and growth. The exception is paddy rice irrigation (Brouwer et al.,  
249 1989), where irrigation was also supplied to keep the upper soil layer saturated. Water demands for  
250 paddy irrigation practices are relatively high compared to conventional irrigation practices due to  
251 increased evaporation and percolation. Therefore, the crop irrigation demands for these two irrigation  
252 practices were calculated and applied separately (i.e. in different sub-grids). Note that multiple cropping

253 seasons are included based on the MIRCA2000 land-use dataset (Portmann et al., 2010) (see  
254 ~~Section~~Sect. 3.1 for more details).

255 Total irrigation demands also included transportation and application losses. Note that transportation  
256 and application losses are not ‘lost’ but rather returned to the soil column without being used by the  
257 crop. The water loss fraction was based on Frenken and Gillet (2012), who estimated the aggregated  
258 irrigation efficiency for 22 United Nations sub-regions. Irrigation efficiencies were estimated based on  
259 the difference between AQUASTAT reported irrigation water withdrawals and calculated irrigation  
260 water requirements (Allen et al., 1998), using data on crop information (e.g. growing season, harvest  
261 area) from AQUASTAT.

### 262 **2.3.2 Domestic and industrial demands**

263 Domestic and industrial water withdrawals were estimated based on Gross Domestic Product (GDP) per  
264 capita and Gross Value Added (GVA) by industries respectively (from Bolt et al. (2018), Feenstra et al.  
265 (2015) and World bank (2010); see Appendix D for more details). These drivers do not fully capture the  
266 multitude of socioeconomic factors that influence water demands (Babel et al., 2007). However, the  
267 wide availability of data allows for extrapolation of water demands to data-scarce regions and future  
268 scenarios (using studies such as Chateau et al. (2014)).

269 Domestic water demands per capita (used for drinking, sanitation, hygiene, and amenity uses) were  
270 estimated similar to Alcamo et al. (2003). Demands increased non-linearly with GDP per capita due to  
271 the acquisition of water using appliances as household become richer. A minimum water supply is  
272 needed for survival, and the saturation of water using appliances sets a maximum on domestic water  
273 demands. Industrial water demands (used for cooling, transportation, and manufacturing) were  
274 estimated similar to Flörke et al. (2013) and Voß and Flörke (2010). Industrial demands increased  
275 linearly with GVA (as an indicator of industrial production). Since industrial water intensities (i.e. the  
276 water use per production unit) vary widely between different industries (Flörke and Alcamo, 2004 ;  
277 Vassolo and Döll, 2005; Voß and Flörke, 2010), the average water intensity was estimated for each

278 country. Both domestic and industrial water demands were also influenced by technological  
279 developments that increase water-use efficiency over time, as in Flörke et al. (2013).

280 Domestic water demands varied monthly based on air temperature variability as in Huang et al. (2018)  
281 (based on Wada et al. (2011b)). Using this approach, water demands were higher in summer than in  
282 winter, especially for counties with strong seasonal temperature differences. Domestic water demand  
283 per capita were downscaled using the HYDE3.2 gridded population maps (Goldewijk et al., 2017).  
284 Industrial water demands were kept constant throughout the year. Industrial demands were downscaled  
285 from national to grid cell values using the NASA Black Marble night-time light intensity map (Roman  
286 et al., 2018). National industrial water demands were allocated based on the relative light intensity per  
287 grid cell for each country.

### 288 2.3.3 Energy and livestock demands

289 Energy water demands (used for cooling of thermoelectric plants) were estimated using data from van  
290 Vliet et al. (2016). Water use intensity for generation (i.e. the water use per generation unit) was  
291 estimated based on the fuel and cooling system type (Goldstein and Smith, 2002), which was combined  
292 with the generation capacity. Note that the data only covered a selection of the total number of  
293 thermoelectric power plants worldwide. Around 27 % of the total (non-renewable) global installed  
294 capacity between 1980 and 2011 was included in the dataset due to lack of information on cooling  
295 system types for the majority of thermoelectric plants. To avoid double counting, energy water demands  
296 were subtracted from the industrial water demands.

297 Livestock water demands (used for drinking and animal servicing) were estimated by combining the  
298 Gridded Livestock of the World (GLW3) map (Gilbert et al., 2018) with the livestock water requirement  
299 reported by ~~Steinfeld et al. (2006)~~Steinfeld et al. (2006). Eight varieties of livestock were considered:  
300 cattle, buffaloes, horses, sheep, goats, pigs, chicken, and ducks. Drinking water demands varied monthly  
301 based on temperature as described by ~~Steinfeld et al. (2006)~~Steinfeld et al. (2006), whereby drinking  
302 water requirements were higher during higher temperatures.

### 303 **3 Model application**

#### 304 **3.1 Setup**

305 VIC-WUR results were generated between 1979 and 2016, excluding a spin-up period of one year  
306 (analysis period from 1980 to 2016). The model used a daily timestep (with a 6-hourly timestep for snow  
307 processes) and simulations were executed on a 0.5° by 0.5° grid (around 55 km at the equator) with three  
308 soil layers per grid cell. Soil and (natural) vegetation parameters were the same as in Nijssen et al.  
309 (2001c) (disaggregated to 0.5°), who used various sources to determine the soil (Cosby et al., 1984;  
310 Carter and Scholes, 1999) and vegetation parameters (Calder, 1993; Ducoudre et al., 1993; Sellers et al.,  
311 1994; Myneni et al., 1997).

312 Nijssen et al. (2001c) used the Advanced Very High Resolution Radiometer vegetation type database  
313 (Hansen et al., 2000) to spatially distinguish 13 land cover types. The land cover type ‘cropland’ in the  
314 original land-cover dataset was replaced by cropland extents from the MIRCA2000 cropland dataset  
315 (Portmann et al., 2010). MIRCA2000 distinguishes the monthly growing area(s) and season(s) of 26  
316 irrigated and rain-fed crop types around the year 2000. Crop types were aggregated into three land cover  
317 types: rain-fed, irrigated, and paddy rice cropland. The natural vegetation was proportionally rescaled  
318 to make up discrepancies between the natural vegetation and cropland extents.

319 Cropland coverage (the cropland area actually growing crops) varied monthly based on the crop growing  
320 areas of MIRCA2000. The remainder was treated as bare soil. Cropland vegetation parameters (e.g. Leaf  
321 Area Index (LAI), displacement, vegetation roughness and albedo) vary monthly based on the crop  
322 growing seasons and the development-stage crop coefficients of the Food and Agricultural Organisation  
323 (Allen et al., 1998).

324 The latest WATCH forcing data Era Interim (aggregated to 6 hourly), developed by the EU Water and  
325 Global Change (WATCH; Harding et al., 2011) project, was used as climate forcing (WFDEI; Weedon  
326 et al., 2014). The dataset provides gridded historical climatic variables of minimum and maximum air  
327 temperature, precipitation (as the sum of snowfall and rainfall, GPCC bias-corrected), relative humidity,  
328 pressure, and incoming shortwave and longwave radiation.

329 For naturalized simulations only the routing module was used. For the human-impact simulations the  
330 sectoral water withdrawals and dam operation modules were turned on in the model simulations. For  
331 the EFR-limited simulations water withdrawals and dam operations were constrained as described.

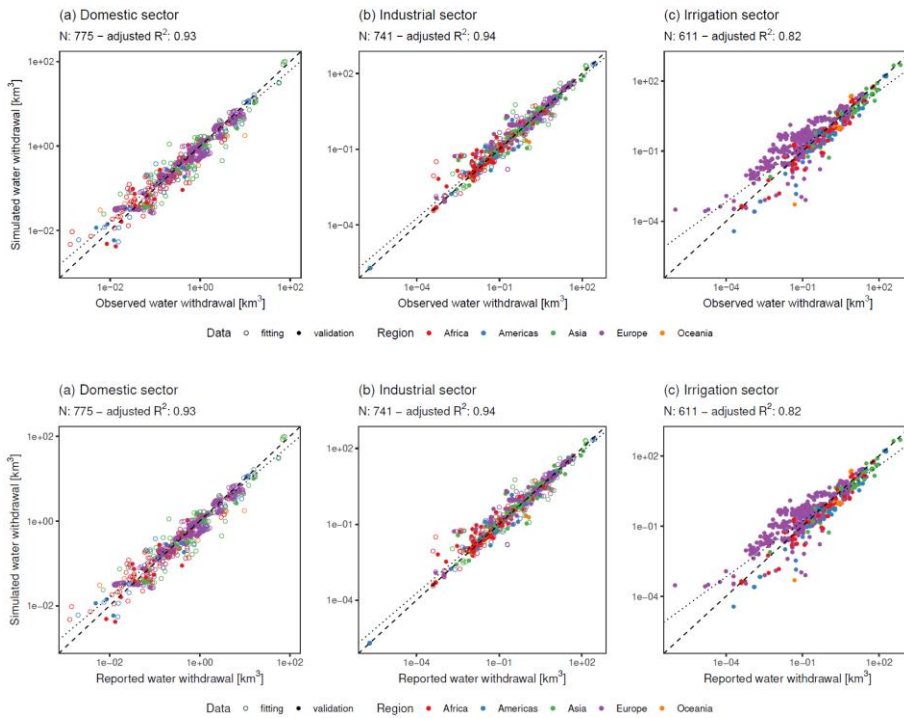
### 332 **3.2 Validation and evaluation**

333 In order to validate the VIC-WUR human-impact modules, water withdrawal, terrestrial total water  
334 storage anomalies, and streamflow and reservoir operation simulations were compared with  
335 observations. The validation specifically focused on the effects of the newly included human-impact  
336 modules, meaning that streamflow and total-water storage anomaly results are shown for river basins  
337 that are strongly influenced by human activities. A general validation for streamflow and terrestrial total  
338 water storage anomalies (including basins with limited human activities) is shown in Appendix E.

#### 339 **3.2.1 Sectoral water withdrawals**

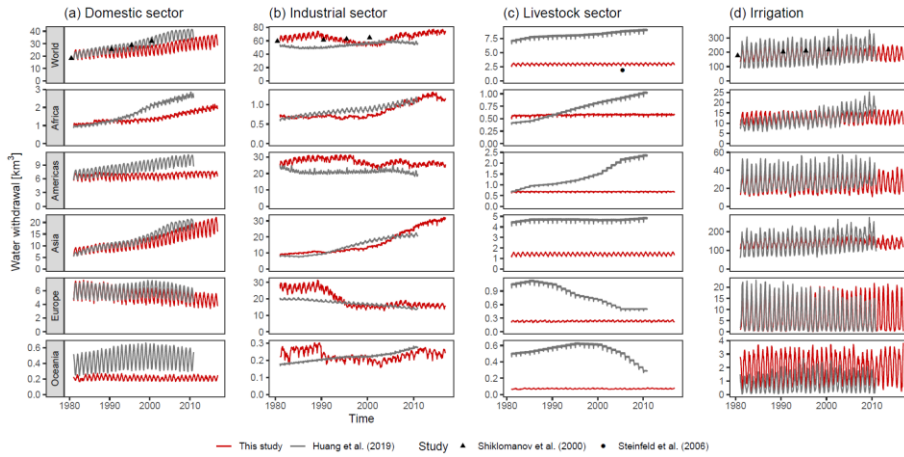
340 Simulated global domestic, industrial, livestock, and irrigation mean water withdrawals were 310, 771,  
341 36, and 2202 km<sup>3</sup> year<sup>-1</sup> respectively for the period of 1980 to 2016. Sectoral water withdrawals were  
342 compared with FAO national annual water withdrawals (FAO, 2016)(FAO, 2016), monthly withdrawal  
343 data from Huang et al. (2018), and annual withdrawal data from Shiklomanov (2000) and ~~Steinfeld et~~  
344 ~~al. (2006)~~Steinfeld et al. (2006). For the latter studies, water withdrawals were aggregated by region  
345 (world, Africa, Asia, Americas, Europe and Oceania). Note that Huang et al. (2018) irrigation water  
346 withdrawals integrate results of four other macro-scale hydrological models (WaterGAP, H08, LPJmL,  
347 PCR-GLOBWB), using the same land-use and climate setup as our study. Results from individual  
348 macro-scale hydrological models are also shown.





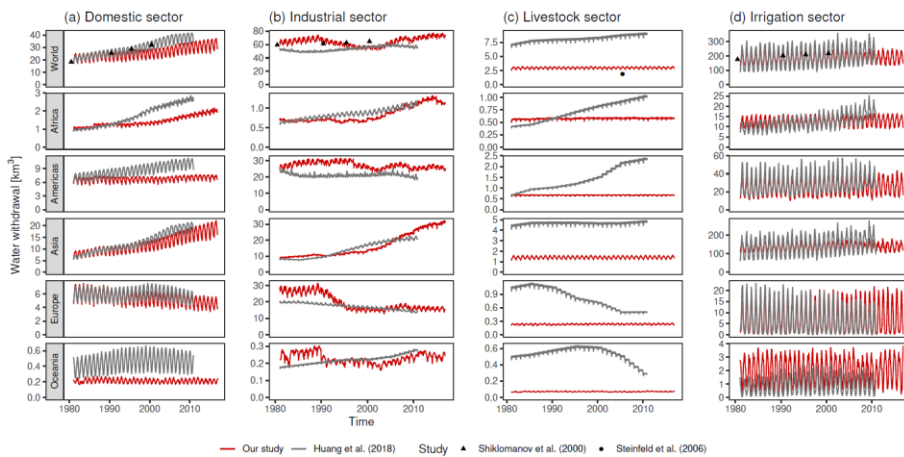
351 **Figure 2: Comparison between simulated and FAO reported national annual water withdrawals for the (a) domestic,**  
 352 **(b) industrial, and (c) irrigation sector. Colours distinguish between regions. Open circles were also used in the**  
 353 **calibration of the water withdrawal demands. The dashed line indicates the 1:1 ratio and the spotted line indicates the**  
 354 **simulated best linear fit. Note the log-log axis which is used to display the wide range of water withdrawals. The  $R^2$**   
 355 **adjusted  $R^2$  is also based on the log values.**

356 Simulated domestic, industrial, and irrigation water withdrawals correlated well to reported national  
 357 water withdrawals, with adjusted  $R^2$  of 0.93, 0.94, and 0.82 for domestic, industrial, and irrigation water  
 358 withdrawal respectively (Figure Fig. 2a-c). Generally, smaller water withdrawals were overestimated  
 359 and larger water withdrawals were underestimated. Differences for the domestic and industrial sector  
 360 were small and probably related to the fact that smaller countries were poorly delineated on a  $0.5^\circ$  by  
 361  $0.5^\circ$  grid. However, irrigation differences were larger with overestimations of irrigation water  
 362 withdrawals in (mostly) Europe. Since irrigation water demands are the results of the simulated water  
 363 balance, overestimations would indicate a regional underestimation of water availability for Europe or  
 364 differences in irrigation efficiency.



365

366 **Figure 3: Comparison between simulated and compiled monthly and annual regional water withdrawals for the (a)**  
 367 **domestic sector, (b) industrial sector, (c) livestock sector, and (d) irrigation. Colours and shapes distinguish between**  
 368 **studies. Note that the jitter in livestock withdrawals is due to the different days per month.**



369

370 **Figure 3: Comparison between simulated and Huang et al. (2018), Shiklomanov (2000), and Steinfeld et al. (2006)**  
 371 **compiled monthly and annual regional water withdrawals for the (a) domestic sector, (b) industrial sector, (c) livestock**  
 372 **sector, and (d) irrigation. Colours and shapes distinguish between studies. Note that the jitter in livestock withdrawals**  
 373 **is due to the different days per month.**

374 When domestic, industrial, and livestock water withdrawals were compared to other studies, results were

375 mixed (Figure 3a-c). Simulated domestic withdrawals followed a similar trend in time. However,

376 simulated domestic water withdrawals trends were overall somewhat underestimated with a mean bias

377 of  $54 \text{ km}^3 \text{ year}^{-1}$  compared to Huang et al. (2018). Asia is the main contributor to the global

378 underestimation, but results are similar in most regions. Simulated industrial water withdrawal were  
 379 (mostly) higher in our study with a mean bias of 107 km<sup>3</sup> year<sup>-1</sup> compared to Huang et al. (2018) but  
 380 only a mean bias of 5 km<sup>3</sup> year<sup>-1</sup> compared to Shiklomanov (2000). Also, industrial water withdrawal  
 381 trends in time were less consistent.

382 Withdrawal differences for the domestic and industrial sector are probably due to the limited data  
 383 availability. Our approach to compute water demands was data-driven and sensitive to data gaps (as  
 384 opposed to Huang et al. (2018) who also combined model results). For example, domestic withdrawal  
 385 data for China was not available before 2007 and industrial withdrawal data was limited before 1990.  
 386 Also, data on the disaggregation of industrial sectors (e.g. energy and mining) was limited, which can  
 387 be important sectors in the water-food-energy nexus.

388 For livestock water withdrawals there is a large discrepancy between the Huang et al. (2018) and  
 389 ~~Steinfeld et al. (2006)~~Steinfeld et al. (2006). Both studies used similar livestock maps, but there was  
 390 large differences in livestock water intensity [litre animal<sup>-1</sup> year<sup>-1</sup>]. Since our study used ~~Steinfeld et al.~~  
 391 ~~(2006)~~Steinfeld et al. (2006) to estimate livestock water intensity, our results were closer to their values  
 392 (slightly higher due to the inclusion of buffaloes, horses, and ducks). Note that Huang et al. (2018) shows  
 393 trends in livestock water withdrawals while our study used static livestock maps.

394 **Table 1: Global Average annual global irrigation water withdrawals as calculated by several global hydrological models.**  
 395 **\*\*\*Includes livestock withdrawals.**

Model	Irrigation withdrawal [km <sup>3</sup> year <sup>-1</sup> ]	Representative years	Reference
VIC-WUR	2202 (± 60)	1980-2016	Our study
H08	(a) 2810	(a) 1995	(a) Hanasaki et al. (2008a)
	(b) 2544 (± 75)	(b) 1984 - 2013	(b) Hanasaki et al. (2018)
MATSIRO	(a) 2158 (± 134)	(a) 1983 - 2007	(a) Pokhrel et al. (2012a)
	(b) 3028 (± 171)	(b) 1998 - 2002	(b) Pokhrel et al. (2015)
LPJmL	2555	1971 - 2000	Rost et al. (2008)
PCR-GLOB	(a) 2644	(a) 2010	(a) Wada and Bierkens (2014)
	(b) 2309 ***	(b) 2000 - 2015	(b) Sutanudjaja et al. (2018)
WaterGAP	(a) 3185	(a) 1998-2002	(a) Döll et al. (2012)

- Formatted: Font: Not Bold
- Formatted: Line spacing: Double
- Formatted: Font: Not Bold, Not Superscript/ Subscript
- Formatted: Font: Not Bold
- Formatted: Font: Not Bold, Not Superscript/ Subscript
- Formatted Table
- Formatted: Font: Not Bold

- Formatted: English (United Kingdom)
- Formatted: English (United Kingdom)
- Formatted: English (United Kingdom)



Formatted: English (United Kingdom)

Formatted: English (United Kingdom)

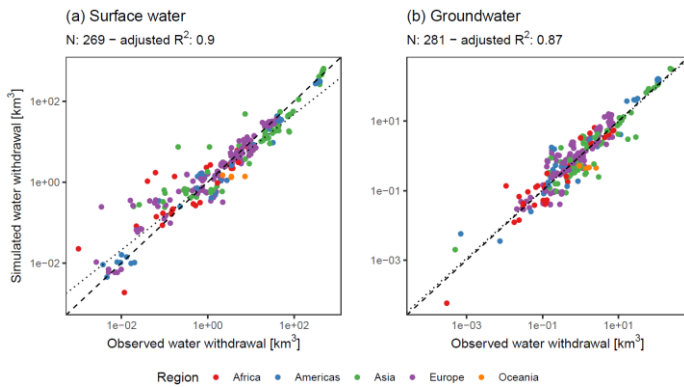
Formatted: English (United Kingdom)

Formatted: English (United Kingdom)

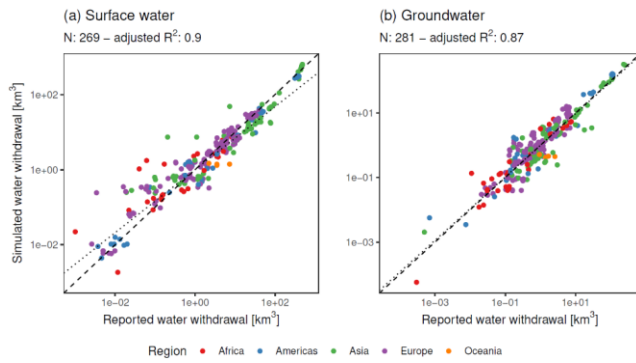
396 Simulated irrigation water withdrawals were within range of other macro-scale hydrological model  
 397 estimates (Table 1). Simulated monthly variability in irrigation water withdrawals is reduced compared  
 398 to the compiled results of Huang et al. (2018) (FigureFig. 3d), especially in Asia. Also, trends in time  
 399 are less pronounced as can be seen in Africa. These differences may indicate a relative low  
 400 weather/climate sensitivity of evapotranspiration in VIC-WUR, as annual and interannual weather  
 401 changes affect irrigation water demands to a lesser degree.

### 402 3.2.2 Groundwater withdrawals and depletion

403 Simulated global mean withdrawals were 2327 and 992 km<sup>3</sup> year<sup>-1</sup> for surface and groundwater  
 404 respectively for the period of 1980 to 2016. Of the global groundwater withdrawals, 334 km<sup>3</sup> year<sup>-1</sup>  
 405 contributed to groundwater depletion. Simulated ground and surface water withdrawals and terrestrial  
 406 total water storage anomalies were compared FAO national annual water withdrawals (FAO,  
 407 2016)(FAO, 2016) and monthly storage anomaly data from the GRACE satellite (NASA, 2002)(NASA,  
 408 2002). GRACE satellite total water storage anomalies were used to validate total water storage dynamics  
 409 as well as groundwater exploitation contributing to downward trends in total water storage. Groundwater  
 410 depletion results from other macro-scale hydrological models are shown as well. In order to compare  
 411 the simulation results to the GRACE dataset, a 300km gaussian filter was applied to the simulated data  
 412 (similar to Long et al. (2015)).



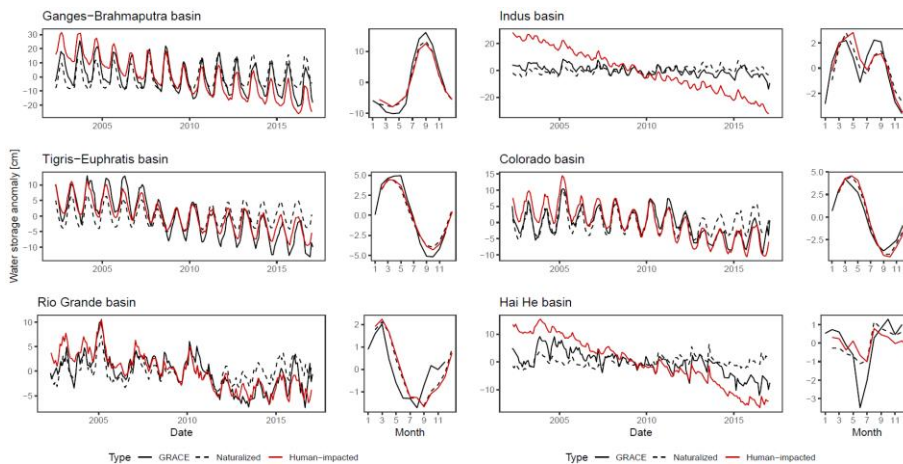
413



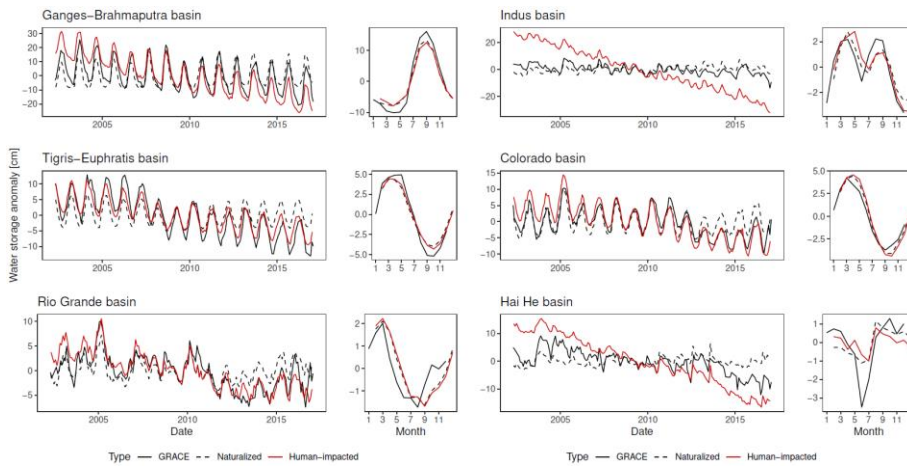
414

415 **Figure 4: Comparison between simulated and FAO reported national annual water withdrawals from (a) surface water**  
 416 **and (b) groundwater. Colours distinguish between regions. The dashed line indicates the 1:1 ratio and the spotted line**  
 417 **indicates the simulated best linear fit. Note the log-log axis which is used to display the wide range of water withdrawals.**  
 418 **The  $R^2$ -adjusted  $R^2$  is also based on the log values.**

419 Simulated surface and groundwater withdrawals correlated well to the reported national water  
 420 withdrawals, with adjusted  $R^2$  of 0.90 and 0.87 for surface and groundwater respectively (FigureFig. 4a-  
 421 b). Surface water withdrawals were overestimated for low withdrawals and underestimated for large  
 422 withdrawals. There is a weak correlation (-0.35) between the underestimations in surface water  
 423 withdrawals and the overestimation in groundwater withdrawals, meaning water withdrawal differences  
 424 could be related to the partitioning between surface and groundwater resources. Also, it is likely that  
 425 low water demands are overestimated (as discussed in SectionSect. 3.2.1), resulting in an overestimation  
 426 of low surface water withdrawals.



427



428  
 429 **Figure 5: Comparison between simulated and GRACE observed monthly terrestrial total water storage anomalies.**  
 430 **Figures indicate timeseries and multi-year mean average for naturalized simulations (dashed), human-impacted**  
 431 **simulations (red), and observed (black) terrestrial total water storage anomalies.**

432 Simulated monthly terrestrial water storage anomalies correlated well to the GRACE observations, with  
 433 mean annual and inter-annual Root Mean Squared Error (RMSE) of 1.9 mm and 3.5 mm respectively.  
 434 The difference between annual and inter-annual performance was primarily due to the groundwater  
 435 depletion process (FigureFig. 5). Simulated groundwater depletion was (mostly) overestimated (e.g.  
 436 Indus and Hai He basins), with higher declining trends in terrestrial total water storage for most basins.  
 437 However, compared to other macro-scale hydrological models, simulated groundwater withdrawal and  
 438 exploitation was within range (Table 2), even though total groundwater withdrawals were relatively  
 439 high.

440 ~~As with the FAO comparison, these results seems to indicate that withdrawal partitioning towards~~  
 441 ~~groundwater is overestimated. However, conclusions regarding groundwater depletion are limited by~~  
 442 ~~the relatively simplistic approach to groundwater used in our study (as discussed by Konikow (2011)~~  
 443 ~~and de Graaf et al. (2017)). For example, processes such as wetland recharge and groundwater flows~~  
 444 ~~between cells are not simulated, even though these could decrease groundwater depletion.~~

445 **Table 2: GlobalAverage annual global groundwater withdrawals and depletion as calculated by several global**  
 446 **hydrological models.**

Model	Groundwater withdrawal [km <sup>3</sup> year <sup>-1</sup> ]	Groundwater depletion [km <sup>3</sup> year <sup>-1</sup> ]	Representative years	Reference
VIC-WUR	992 (± 51)	316 (± 63)	1980 - 2016	Our study
H08	789 (± 30)	182 (± 26)	1984 - 2013	Hanasaki et al. (2018)
MATSIRO	570 (± 61)	330	1998 - 2002	Pokhrel et al. (2015)
GCAM		(a) 600	(a) 2005	(a) Kim et al. (2016)
		(b) 550	(b) 2000	(b) Turner et al. (2019)
PCR-GLOB	(a) 952	(a) 304	(a) 2010	(a) Wada and Bierkens (2014)
	(b) 632	(b) 171	(b) 2000 - 2015	(b) Sutanudjaja et al. (2018)
WaterGAP	(a) 1519	(a) 250	(a) 1998-2002	(a) Döll et al. (2012)
	(b) 888	(b) 113	(b) 2000 - 2009	(b) Döll et al. (2014)

As with the FAO comparison, these results seems to indicate that withdrawal partitioning towards groundwater is overestimated. However, conclusions regarding groundwater depletion are limited by the relatively simplistic approach to groundwater used in our study (as discussed by Konikow (2011) and de Graaf et al. (2017)). For example, processes such as wetland recharge and groundwater flows between cells are not simulated, even though these could decrease groundwater depletion.

### 3.2.3 Discharge modification

Simulated discharge was compared to GRDC station data (GRDC, 2003) for various human-impacted rivers. Stations were selected if the upstream area was larger than 20,000 km<sup>2</sup>, matched the simulated upstream area at the station location, and the available data spanned more than 2 years. Subsequently, stations where the human-impact modules did not sufficiently impacted discharge were omitted. In order to validate the reservoir operation more thoroughly, simulated reservoir inflow, storage, and release was compared with operation data from Hanasaki et al. (2006) and Yassin et al. (2019). Reservoirs were included if the simulated storage capacity (which is the combined storage capacity of all large dams in a grid) was similar to observed storage capacity.

Formatted: Font: 9 pt, Not Bold

Formatted Table

Formatted: Font: 9 pt

Formatted: Font: 9 pt

Formatted: Font: 9 pt

Formatted: Font: 9 pt

Formatted: Font: 9 pt

Formatted: Font: 9 pt

Formatted: Font: 9 pt

Formatted: Font: 9 pt

Formatted: Font: 9 pt

Formatted: Font: 9 pt

Formatted: Font: 9 pt

Formatted: Font: 9 pt

Formatted: Font: 9 pt

Formatted: Font: 9 pt, English (United Kingdom)

Formatted: Font: 9 pt, English (United Kingdom)

Formatted: Font: 9 pt, English (United Kingdom)

Formatted: Font: 9 pt

Formatted: Font: 9 pt

Formatted: Font: 9 pt, English (United Kingdom)

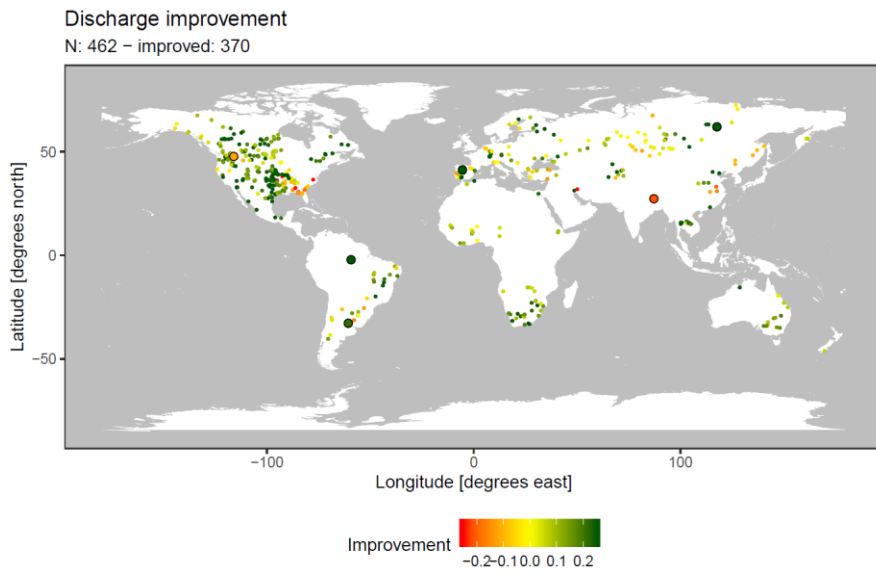
Formatted: Font: 9 pt, English (United Kingdom)

Formatted: Font: 9 pt

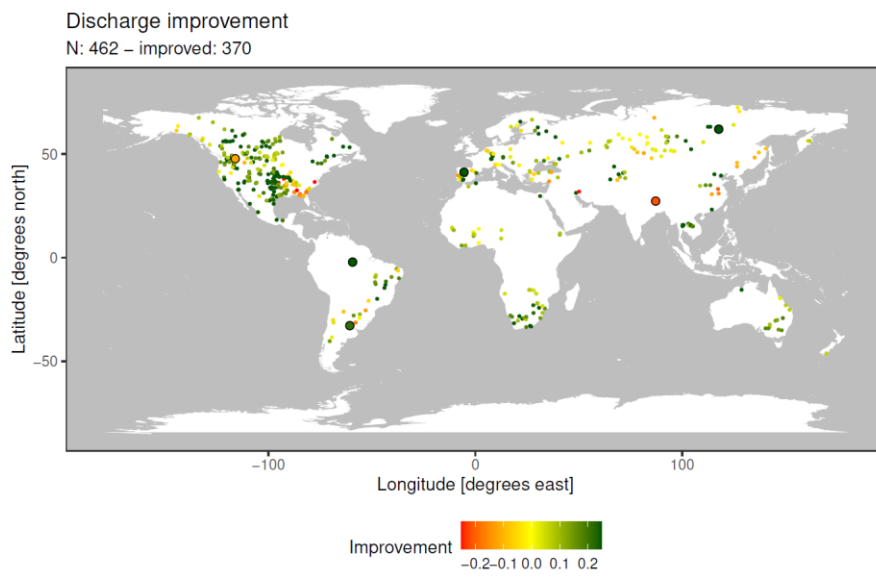
Formatted: Font: 9 pt

Formatted: Font: 9 pt

Formatted: Font: 9 pt, English (United Kingdom)



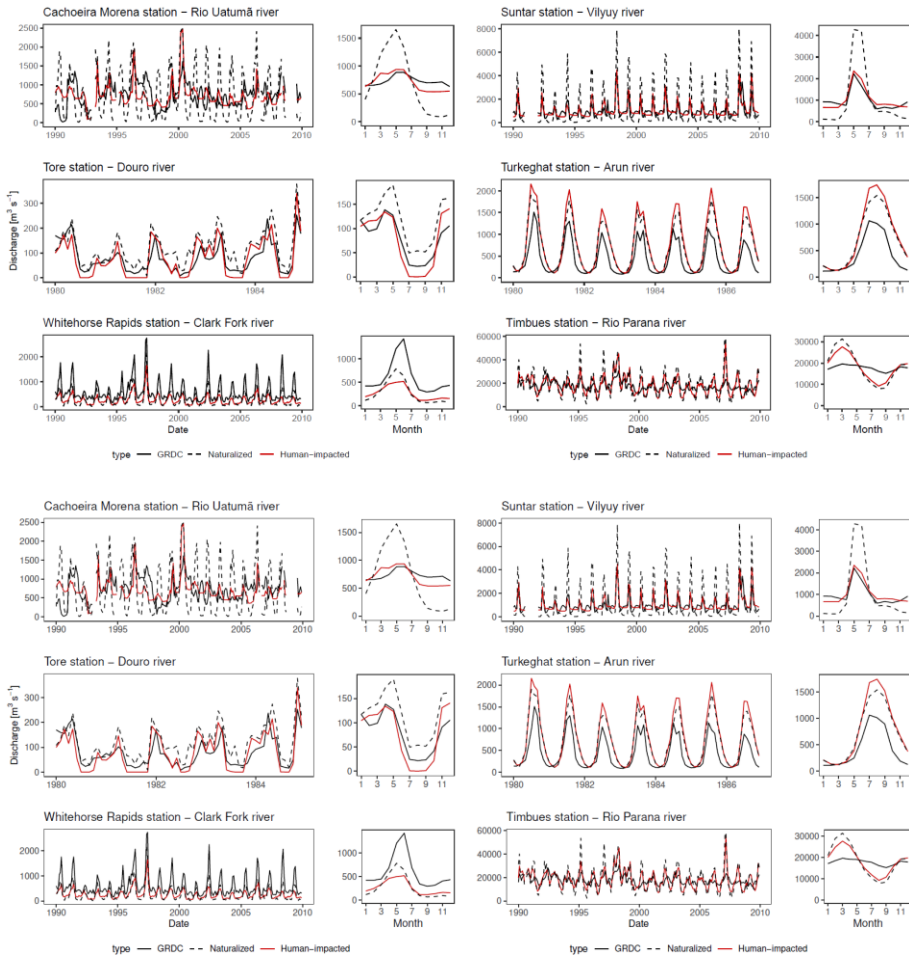
461



462

463 **Figure 6: Discharge improvement from naturalized to human-impacted simulations (as a fraction of the naturalized**  
 464 **RMSE). Circled larger stations are shown in [Figure Fig. 7](#).**





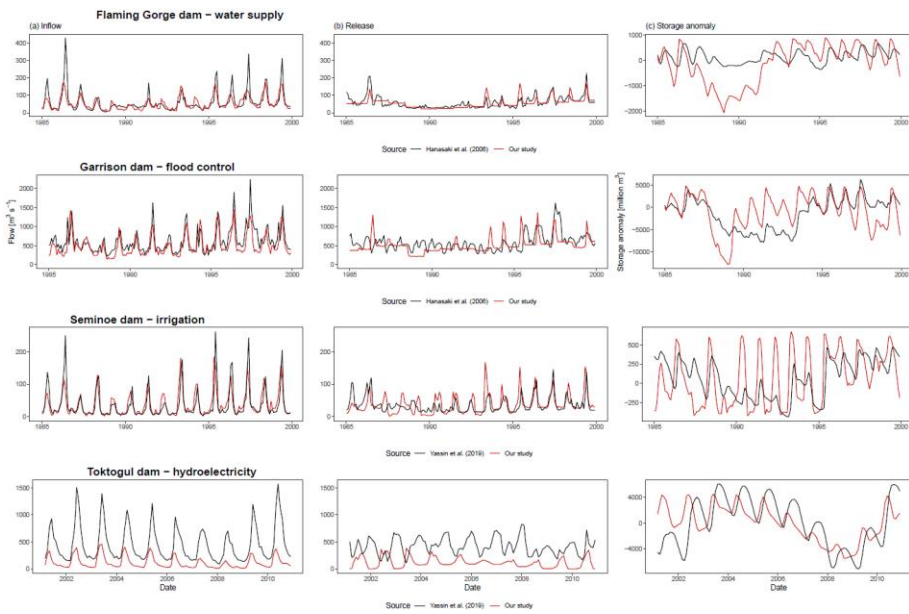
465

466

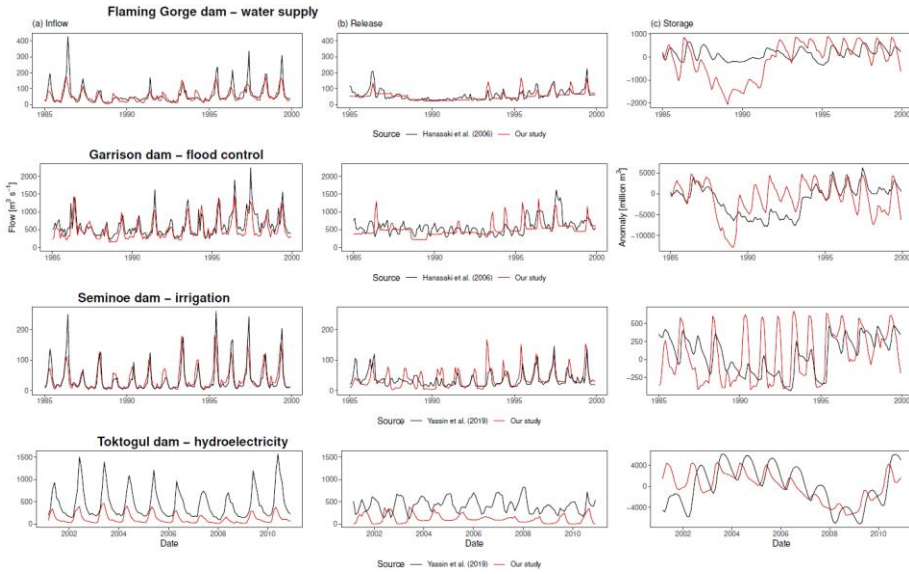
467 **Figure 7: Comparison between simulated and GRDC observed discharge. Figures indicate timeseries and multi-year**  
 468 **average of for naturalized simulations (dashed), human-impacted simulations (red), and observed (black) discharge.**

469 The inclusion of the human-impact modules improved discharge performance, measured in RMSE, for  
 470 370 out of 462 stations (80 %; [Figure Fig. 6 and 7](#)). Improvements were mainly due to the effects of  
 471 reservoir operation on discharges (e.g. Cachoeira Morena and Suntar stations), but also due to  
 472 withdrawal reductions (e.g. Tore station). Reservoir effects on discharge were sometimes  
 473 underestimated however (e.g. Timbues station).

474 Decreased performance was mostly related to under or overestimations of (calibrated) natural  
 475 streamflow which was subsequently exacerbated by reservoir operation and water withdrawals. For  
 476 example, the Clark Fork river naturalized streamflow was underestimated, which was subsequently  
 477 further underestimated by the human-impact modules (Whitehorse Rapids station). Also, increases in  
 478 discharge due to groundwater withdrawals could increase naturalized streamflow (e.g. Turkeghat  
 479 station). Further improvements to discharge performance would most likely require either a recalibration  
 480 of the VIC model parameters.



481



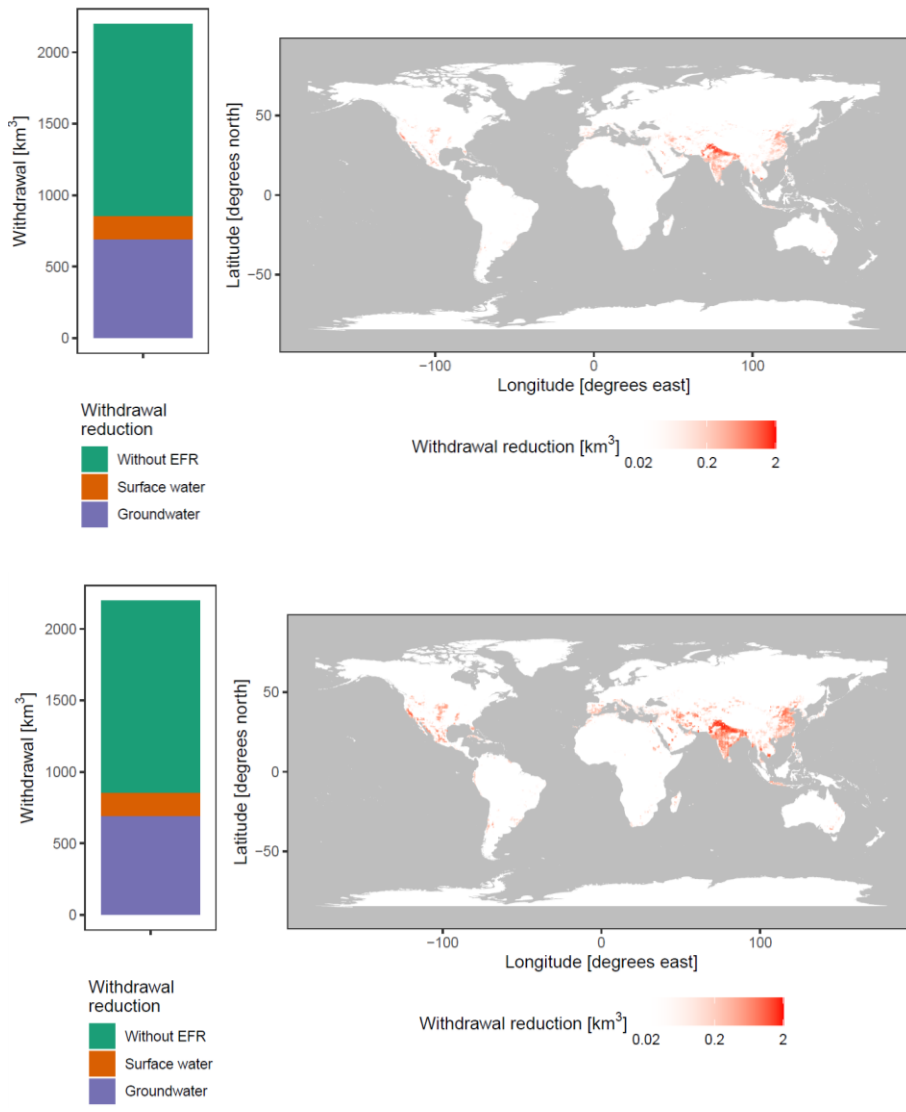
482

483 **Figure 8: Comparison between simulated and [Hanasaki et al. \(2006\)](#) and [Yassin et al. \(2019\)](#) observed reservoir**  
 484 **operation. Figures indicate timeseries and multi-year averages of (a) inflow, (b) release, and (c) storage anomalies for**  
 485 **human-impacted simulations (red) and observations (black).**

486 For individual reservoirs, operation characteristics were generally well simulated ([FigureFig. 8](#)), with  
 487 reductions in annual discharge variations (e.g. Flaming Gorge and Garrison dams) and increased water  
 488 release for irrigation (e.g. Seminoe dam). However, due to changes in locally simulated and actual  
 489 inflow, dam operation can take on different characteristics (e.g. Toktogul dam). Also, peak discharge  
 490 events caused by reservoir overflow (as also described by [Masaki et al. \(2018\)](#)) were not always  
 491 sufficiently represented in the observations (e.g. Garrison dam). These differences indicate locally  
 492 varying reservoir operation strategies. Several studies have developed reservoir operation schemes that  
 493 can be calibrated to the local situation ([Rougé et al., 2019](#); [Yassin et al., 2019](#)). However, worldwide  
 494 implementations of these operation schemes remains limited by data availability.

### 495 3.3 Integrated environmental flow requirements

496 In order to assess the impact and capabilities of the newly integrated environmental flow requirements  
 497 (EFRs) module, simulated water withdrawals with and without adhering to EFRs were compared.



498

499

500 **Figure 9: Average annual irrigation water withdrawal reductions when adhering to EFRs as (left) global gross total**  
 501 **(left) and (right) spatially distributed; (right).** Global gross totals are separated into withdrawals without any reduction  
 502 (green), surface water withdrawal reductions (orange), and groundwater withdrawal reductions (purple). Note the log  
 503 axis for the spatially distributed withdrawal reductions to better display the spatial distribution of the reductions.

504 If water-use would be limited to EFRs, irrigation withdrawals would need to be reduced by about 39 %

505 (851 km<sup>3</sup> year<sup>-1</sup>) (Figure Fig. 9a). Under the strict requirements used in our study, 81 % (693 km<sup>3</sup> year

506 <sup>1)</sup> of the reduction could be attributed to limitations imposed on groundwater withdrawals. Subsequently,  
507 the impact of the environmental flow requirements (if adhered to) would be largest in groundwater  
508 dependent regions (Figure 9b). Note that, due to the full integration of EFRs, downstream surface  
509 water withdrawals increased by 98 km<sup>3</sup> year<sup>-1</sup> when limiting groundwater withdrawals on top of limiting  
510 surface water withdrawals, due to increase subsurface runoff.

511 Reductions due to EFRs were similar to Jägermeyr et al. (2017), who calculated irrigation withdrawal  
512 reductions of 41 % (997 km<sup>3</sup> year<sup>-1</sup>) assuming only surface water abstractions. In our study, surface  
513 water reductions were smaller since the strict groundwater requirements increases subsurface runoff to  
514 surface waters. It can be discussed to what extent the EFRs for baseflow were too constricting, since  
515 they were based on the relatively stringent EFR for streamflow of Richter et al. (2012) (10 % of the  
516 natural streamflow). However, in the absence of any other standards, this baseflow standard remains the  
517 best available. Note that, even when accounting for EFRs for baseflow on a grid scale, withdrawals  
518 could still have local and long-term impacts that are not captured by the model. The timing, location,  
519 and depth of groundwater withdrawals are important factors due to their interactions with the local  
520 geohydrology, as discussed by Gleeson and Richter (2018).

#### 521 **4 Conclusion**

#### 522 **4 Conclusions**

523 The VIC-WUR model introduced in this paper aims to provide new opportunities for global water  
524 resource assessments using the VIC model. Accordingly, several anthropogenic impact modules, based  
525 on previous major works, were integrated into the VIC-5 macro-scale hydrological model: domestic,  
526 industrial, energy, livestock, and irrigation water withdrawals from both surface water and groundwater  
527 as well as an integrated environmental flow requirement module and dam operation module. Global  
528 gridded datasets on domestic, industrial, energy, and livestock demand were developed separately and  
529 used to force the VIC-WUR model.

530 Simulated national water withdrawals were in line with reported national annual withdrawals ( $R^2$   
531 adjusted  $R^2 > 0.8$ ; both per sector as per source). However, the data-oriented methodology used to derive  
532 sectoral water demands resulted in different withdrawal trends over time compared to other studies  
533 (Shiklomanov, 2000; Huang et al., 2018). While the current setup to estimate sectoral water demands is  
534 well suited for future water withdrawal estimations, there are various other approaches (e.g. Alcamo et  
535 al., 2003; Vassolo and Döll, 2005; Shen et al., 2008; Hanasaki et al., 2013; Wada and Bierkens, 2014).  
536 As the model setup of VIC-WUR allows for the evaluation of other sectoral water demand inputs (on  
537 various temporal aggregations), several different approaches can be used depending on the focus region  
538 and data-availability for calibration. Terrestrial water storage anomaly trends were well simulated (mean  
539 annual and inter-annual RMSE of 1.9 mm and 3.6 mm respectively), while groundwater exploitation  
540 was overestimated. Overestimated groundwater depletion rates are likely related to an over-partitioning  
541 of water withdrawals to groundwater. The implemented human impact modules increased simulated  
542 discharge performance (370 out of 462 stations), mostly due to the effects of reservoir operation.

543 An assessment of the effect of EFRs shows that, when one would adhere to these requirements, global  
544 water withdrawals would be severely limited (39 %). This limitation is especially the case for  
545 groundwater withdrawals, which, under the strict requirements used in our study, need to be reduced by  
546 81 %.

547 VIC-WUR has potential for studying impacts of climate change and anthropogenic developments on  
548 current and future water resources and sectoral specific-water scarcity. The additions presented here  
549 make the VIC model more suited for fully-integrated worldwide water-resource assessments and  
550 substantially decrease computation times compared to Haddeland et al. (2006a).

## 551 **5 Appendices**

### 552 ~~5.1 Code availability~~

553 ~~All code for the VIC-WUR model is freely available at [github.com/wur-wag/VIC](https://github.com/wur-wag/VIC) (tag VIC-WUR-2.1.0;  
554 [DOI-10.5281/zenodo.3934325](https://doi.org/10.5281/zenodo.3934325)) under the GNU General Public License, version 2 (GPL-2.0). VIC~~

555 ~~WUR documentation can be found at [view.wur.readthedocs.io](http://view.wur.readthedocs.io). The original VIC model is freely available~~  
556 ~~at [github.com/UW-Hydro/VIC](https://github.com/UW-Hydro/VIC) (tag VIC.5.0.1; DOI 10.5281/zenodo.267178) under the GNU General~~  
557 ~~Public License, version 2 (GPL 2.0). VIC documentation can be found at [vic.readthedocs.io](http://vic.readthedocs.io).~~  
558 ~~Documentation and scripts concerning input data used in our study is freely available at~~  
559 ~~[github.com/brandt/VIC\\_support](https://github.com/brandt/VIC_support) (tag VIC-WUR.2.1.0; DOI 10.5281/zenodo.3934363) under the GNU~~  
560 ~~General Public License, version 3 (GPL 3.0).~~

## 561 **6 Appendix**

### 562 **6.15.1 Appendix A: VIC water and energy balance**

563 In VIC each sub-grid computes the water and energy balance individually (i.e. sub-grid do not exchange  
564 water or energy between one another). For the water balance, incoming precipitation is partitioned  
565 between evapotranspiration, surface and subsurface runoff, and soil water storage. Potential  
566 evapotranspiration is based on the Penman-Monteith equation without the canopy resistance  
567 (Shuttleworth, 1993). The actual evapotranspiration is calculated by two methods, based on whether the  
568 land cover is vegetated or not (bare soil). Evapotranspiration of vegetation is constrained by stomatal,  
569 architectural and aerodynamic resistances and is partitioned between canopy evaporation and  
570 transpiration based on the intercepted water content of the canopy (Deardorff, 1978; Ducoudre et al.,  
571 1993). Bare soil evaporation is constrained by the saturated area of the upper soil layer. The saturated  
572 area is variable within the grid since (as the model name implies) the infiltration capacity of the soil is  
573 assumed heterogeneous (Franchini and Pacciani, 1991). Saturated areas evaporate at the potential  
574 evaporation rate while in unsaturated areas evaporation is limited. Surface runoff is produced by  
575 precipitation over saturated areas. Precipitation over unsaturated areas infiltrates into the upper soil layer  
576 and drains through the soil layers based on the gravitational hydraulic conductivity equations of ~~Brooks~~  
577 ~~and Corey (1964).Brooks and Corey (1964)~~. In the first and second layer water is available for  
578 transpiration, while the third layer is assumed to be below the root zone. From the third layer baseflow  
579 is generated based on the non-linear Arno conceptualization (Franchini and Pacciani, 1991). Baseflow

580 increases linearly with soil moisture content when the moisture content is low. At higher soil moisture  
581 contents the relation is non-linear, representing subsurface storm-flows.

582 For the energy balance, incoming net radiation is partitioned between sensible, latent, and ground heat  
583 fluxes and energy storage in the air below the canopy. The energy storage below the canopy is omitted  
584 if it is considered negligible (e.g. the canopy surface is open or close to the ground). The latent heat flux  
585 is determined by the evapotranspiration as calculated in the water balance. The sensible heat flux is  
586 calculated based on the difference between the air and surface temperature and the ground heat flux is  
587 calculated based on the difference between the soil and surface temperature. Since the incoming net  
588 radiation is also a function of the surface temperature (specifically the outgoing longwave radiation),  
589 the surface temperature is solved iteratively. Subsurface ground heat fluxes are calculated assuming an  
590 exponential temperature profile between the surface and the bottom of the soil column, where the bottom  
591 temperature is assumed constant. Later model developments included options for finite difference  
592 solutions of the ground temperature profile (Cherkauer and Lettenmaier, 1999), spatial distribution of  
593 soil temperatures (Cherkauer and Lettenmaier, 2003), a quasi-2-layer snow-pack snow model  
594 (Andreadis et al., 2009), and blowing snow sublimation (Bowling et al., 2004).

#### 595 **6.25.2 Appendix B: EFRs for surface and groundwater**

596 VIC-WUR used the Variable Monthly Flow (VMF) method (Pastor et al., 2014) to limit surface water  
597 withdrawals. The VMF method (Pastor et al., 2014) calculates the EFRs for streamflow as a fraction of  
598 the natural flow during high (Eq. A.1), intermediate (Eq. A.2), and low (Eq. A.3) flow periods. The  
599 presumptive standard Gleeson and Richter (2018) is used to limit groundwater withdrawals (including  
600 aquifer groundwater withdrawals). This standard calculates the EFRs for baseflow as 90 % of the natural  
601 subsurface runoff through time (Eq. A.4). Here, daily instead of monthly EFRs were used to better  
602 capture the monthly flow variability.

$$603 \quad EFR_{s,d} = 0.6 \cdot NF_{s,d} \quad \text{Eq. (A.1)}$$

$$604 \quad \text{where } NF_{s,d} \leq 0.4 \cdot NF_{s,y}$$

$$605 \quad EFR_{s,d} = 0.45 \cdot NF_{s,d} \quad \text{Eq. (A.2)}$$



606 *where*  $0.4 \cdot MF_{s,y} < NF_{s,d} \leq 0.8 \cdot NF_{s,y}$

607  $EFR_{s,d} = 0.3 \cdot NF_{s,d}$  Eq. (A.3)

608 *where*  $NF_{s,d} > 0.8 \cdot NF_{s,y}$

609  $EFR_{b,d} = 0.9 \cdot NF_{b,d}$  Eq. (A.4)

610 Where  $EFR_{s,d}$  is the daily EFRs for streamflow [ $m^3 s^{-1}$ ],  $EFR_{b,d}$  the daily EFRs for baseflow [ $m^3 s^{-1}$ ],  
611  $NF_{s,d}$  is the average natural daily streamflow [ $m^3 s^{-1}$ ], and  $NF_{s,y}$  is the average natural yearly streamflow  
612 [ $m^3 s^{-1}$ ], and  $NF_{b,d}$  is the average natural daily baseflow [ $m^3 s^{-1}$ ].

613 EFRs for streamflow and baseflow were based on VIC-WUR naturalized simulations between 1980 and  
614 2010. Average natural daily flows were calculated as the interpolated multi-year monthly average flow  
615 over the simulation period.

### 616 **6.3.5.3 Appendix C: Dam operation scheme**

617 VIC-WUR used a dam operation scheme based on Hanasaki et al. (2006). Target release (i.e. the  
618 estimated optimal release) was calculated at the start of the operational year. The operational year starts  
619 at the month where the inflow drops below the average annual inflow, and thus the storage should be at  
620 its desired maximum. The scheme distinguished between two dam types: (1) dams that did not account  
621 for water demands downstream (e.g. hydropower dams or flood control) and (2) dams that did account  
622 for water demands downstream (e.g. irrigation dams). The original scheme of Hanasaki et al. (2006)  
623 also accounts for EFRs, which were fixed at half the annual mean inflow. Other studies lowered the  
624 requirements to a tenth of the mean annual inflow, increasing irrigation availability and preventing  
625 excessive releases (Biemans et al., 2011; Voisin et al., 2013b). In our study the original dam operation  
626 scheme was adapted slightly to account for monthly varying EFRs.

627 For dams that did not account for demands, the initial release was set at the mean annual inflow corrected  
628 by the variable EFRs (Eq. A.5). For dams that did account for demands, the initial release was increased  
629 during periods of higher water demand. If demands were relatively high compared to the annual inflow,  
630 the release was corrected by the demand relative to the mean demand (Eq. A.6). If demands were

631 relatively low compared to the annual inflow, release was corrected based on the actual water demand  
632 (Eq. A.7).

633

$$634 \quad R'_m = EFR_{s,m} + (I_y - EFR_{s,y}) \quad \text{Eq. (A.5)}$$

635 *where*  $D_y = 0$

$$636 \quad R'_m = EFR_{s,m} + (I_y - EFR_{s,y}) * \frac{D_m}{D_y} \quad \text{Eq. (A.6)}$$

637 *where*  $D_y > 0$  and  $D_y > (I_y - EFR_{s,y})$

$$638 \quad R'_m = EFR_{s,m} + (I_y - EFR_{s,y}) - D_y + D_m \quad \text{Eq. (A.7)}$$

639 *where*  $D_y > 0$  and  $D_y \leq (I_y - EFR_{s,y})$

640 Where  $R'_m$  is the initial monthly target release [ $\text{m}^3 \text{s}^{-1}$ ],  $EFR_{s,m}$  is the average monthly EFR for  
641 streamflow demand [ $\text{m}^3 \text{s}^{-1}$ ],  $I_y$  is the average yearly inflow [ $\text{m}^3 \text{s}^{-1}$ ],  $EFR_{s,y}$  is the average yearly EFR  
642 for streamflow [ $\text{m}^3 \text{s}^{-1}$ ],  $D_m$  is the average monthly water demand [ $\text{m}^3 \text{s}^{-1}$ ], and  $D_y$  is the average yearly  
643 water demand [ $\text{m}^3 \text{s}^{-1}$ ].

644 As in Hanasaki et al. (2006), the initial target release was adjusted based on storage and capacity. Target  
645 release was adjusted to compensate differences between the current storage and the desired maximum  
646 storage (Eq. A.8). Target release was additionally adjusted if the storage capacity is relatively low  
647 compared to the annual inflow, and unable to store large portions of the inflow for later release (Eq.  
648 A.9).

$$649 \quad R_m = k \cdot R'_m \quad \text{Eq. (A.8)}$$

650 *where*  $c \geq 0.5$

$$651 \quad R_m = \left(\frac{c}{0.5}\right)^2 \cdot k \cdot R'_m + \left\{1 - \left(\frac{c}{0.5}\right)^2\right\} \cdot I_m \quad \text{Eq. (A.9)}$$

652 *where*  $0 \leq c \leq 0.5$

653 Where  $I_m$  is the average monthly inflow [ $\text{m}^3 \text{s}^{-1}$ ],  $c$  the capacity parameter [-] calculated as the storage  
 654 capacity divided by the mean annual inflow, and  $k$  the storage parameter [-] calculated as current storage  
 655 divided by the desired maximum storage. The desired maximum storage was set at 85 % of the storage  
 656 capacity as recommended by Hanasaki et al. (2006).

657 Water inflow, demand and EFRs were estimated based on the average of the past five years. Water  
 658 demands were based on the water demands of downstream cells. Only a fraction of water demands were  
 659 taken into account, based on the fraction of discharge the dam controlled. For example: if a dam  
 660 controlled 70 % of the discharge of a downstream cell, than 70 % of its demands were taken into account.  
 661 Fractions smaller than 25 % were ignored.

662 The original dam operation scheme of Hanasaki et al. (2006) was shown to produce excessively high  
 663 discharge events due to overflow releases (Masaki et al., 2018). These overflow releases occurred due  
 664 to a mismatch between the expected and actual inflow. In our study, dam release was increased during  
 665 high-storage events to prevent overflow and accompanying high discharge events. If dam storage was  
 666 above the desired maximum storage, target dam release was increased to negate the difference (Eq.  
 667 A.10). If dam storage was below the desired minimum storage, release is decreased (Eq. A.11). Dam  
 668 release was adjusted exponentially based on the relative storage difference: small storage differences  
 669 were only corrected slightly, but if the dam was close to overflowing or emptying, the difference was  
 670 corrected strongly.

$$671 \quad R_a = R_m + \frac{(S-C\alpha)}{\gamma} \cdot \left( \frac{\frac{S}{C} - \alpha}{1-\alpha} \right)^b \quad \text{Eq. (A.10)}$$

672 where  $S > C\alpha$

$$673 \quad R_a = R_m + \frac{(S-C(1-\alpha))}{\gamma} \cdot \left( \frac{(1-\alpha) - \frac{S}{C}}{1-\alpha} \right)^b \quad \text{Eq. (A.11)}$$

674 where  $S < C(1-\alpha)$

675 Where  $R_a$  is the actual dam release [ $\text{m}^3 \text{s}^{-1}$ ],  $S$  the dam storage capacity [ $\text{m}^3$ ],  $\alpha$  the fraction of the capacity  
 676 that is the desired maximum [-],  $\beta$  the exponent determining the correction increase [-], and  $\gamma$  the

Formatted: Font: Italic  
 Formatted: Font: Italic  
 Formatted: Font: Italic  
 Formatted: Font: Italic  
 Formatted: Font: Italic

677 parameter determining the period when the release is corrected [ $s^{-1}$ ]. In testing the exponent and period  
678 were tuned to 0.6 and 5 days respectively.

## 679 **6.4.5.4 Appendix D: Water demand**

### 680 **6.4.5.4.1 Fitting and validation data**

681 Data on irrigation, domestic, and industrial water withdrawals were based on the AQUASTAT database  
682 (~~FAO, 2016~~)(FAO, 2016), EUROSTAT database (~~EC, 2019~~)(EC, 2019) and United Nations World  
683 Water Development Report (Connor, 2015). Data on GDP per capita and GVA ~~was~~were abstracted from  
684 the Maddison Project Database 2018 (Bolt et al., 2018), Penn World Table 9.0 (Feenstra et al., 2015)  
685 and World Bank Development Indicators (World bank, 2010).

686 Available data for domestic and industrial withdrawals were divided into a dataset used for parameter  
687 fitting (80 %) and a dataset used for validation (20 %). Domestic water demands were estimated for  
688 each United Nations sub-region, and thus the data was divided per sub-region to ensure a good global  
689 coverage of data. In the same manner industrial water demand were divided per country. In case there  
690 is only a single data ~~point~~entry, the ~~data~~entry was added to both the fitting and validation data.

### 691 **6.4.5.4.2 Irrigation sector**

692 Conventional irrigation demands were calculated when soil moisture contents drop below the critical  
693 threshold where evapotranspiration will be limited. Demands were set to relieve water stress (Eq. A.12).  
694 Paddy irrigation demands were set to always keep the soil moisture content of the upper soil layer  
695 saturated (Eq. A.13), similar to Hanasaki et al. (2008b) and Wada et al. (2014). For paddy irrigation, the  
696 saturated hydraulic conductivity of the upper soil layer was reduced by its cubed root to simulate  
697 puddling practices, as recommended by the CROPWAT model (~~Smith, 1996~~)(Smith, 1996). Total  
698 irrigation demands were adjusted by the irrigation efficiency (Eq. A.14). Paddy irrigation used an  
699 irrigation efficiency of 1 since the water losses were already incorporated in the water demand  
700 calculation.

$$701 ID'_{conventional} = (W_{cr,1} + W_{cr,2}) - (W_1 + W_2) \quad \text{Eq. (A.12)}$$

$$702 \quad \text{where } W_1 + W_2 < W_{cr,1} + W_{cr,2}$$

703  $ID'_{paddy} = W_{max,1} - W_1$  Eq. (A.13)

704 where  $W_1 < W_{max,1}$

705  $ID = ID' * IE$  Eq. (A.14)

706 Where  $ID'_{conventional}$  is the conventional crop irrigation demand [mm],  $ID'_{paddy}$  is the paddy crop irrigation  
 707 demand [mm],  $ID$  is the total irrigation demand [mm],  $W_1$  and  $W_2$  are the soil moisture contents of the  
 708 first and second soil layer respectively [mm],  $W_{cr}$  is the critical soil moisture content [mm],  $W_{max}$  the  
 709 maximum soil moisture content [mm], and  $IE$  is the irrigation efficiency [mm mm<sup>-1</sup>].

710 **6.4.3.5.4.3 Domestic sector**

711 Domestic water demands were represented by using a sigmoid curve for the calculation of structural  
 712 domestic water demands (Eq.A.15) and a efficiency rate for the calculation of water-use efficiency  
 713 increases (Eq. A.16). These equations differ slightly from Alcamo et al. (2003) since our study used the  
 714 base 10 logarithms of GDP and water withdrawals per capita as they provided a better fit.

715  $DSW_y = DSW_{min} + (DSW_{max} - DSW_{min}) * \frac{1}{1 + e^{-f(GDP_y - o)}}$  Eq. (A.15)

716  $DW_y = 10^{DSW_y} \cdot TE^{y - y_{base}}$  Eq. (A.16)

717 Where  $DSW$  is the yearly structural domestic withdrawal [ $\log_{10} \text{ m}^3 \text{ cap}^{-1}$ ],  $DW$  the yearly domestic  
 718 withdrawal [ $\text{m}^3 \text{ cap}^{-1}$ ],  $DSW_{min}$  the minimum structural domestic withdrawal [ $\log_{10} \text{ m}^3 \text{ cap}^{-1}$ ],  
 719  $DSW_{max}$  the maximum structural domestic withdrawal (without technological improvement)  
 720 [ $\log_{10} \text{ m}^3 \text{ cap}^{-1}$ ],  $GDP$  the yearly gross domestic product [ $\log_{10} \text{ USD}_{equivalent} \text{ cap}^{-1}$ ],  $f$  [-] and  $o$  [ $\log_{10}$   
 721  $\text{USD}_{equivalent}$ ] the parameters that determine the range and steepness of the sigmoid curve,  $y$  the year  
 722 index,  $TE$  the technological efficiency rate [-], and  $y_{base}$  the base year (taken to be 1980).

723  $DSW_{min}$  was set at  $7.5 \text{ l cap}^{-1} \text{ d}^{-1}$  based on the World Health Organisation standard (Reed and Reed, 2013),  
 724  $DSW_{max}$  was estimated at around  $450 \text{ l cap}^{-1} \text{ y}^{-1}$  based on a global curve fit, and  $TE$  was set at 0.995, 0.99,  
 725 and 0.98 for developing, transition and developed countries respectively (United Nations development  
 726 status classification) based on Flörke et al. (2013). Curve parameters  $f$  and  $o$  were estimated for the 23  
 727 United Nations sub-regions based on the GDP per capita and domestic water withdrawal data. In case

728 insufficient data was available to calculate parameters values, regional (4 sub-regions) or global (4 sub-  
729 regions) parameter estimates were used.

#### 730 **6.4.45.4.4 Industrial sector**

731 Industrial water demands were represented by using a linear formula for the calculation of structural  
732 industrial water demands (Eq. A.17) and a efficiency rate for the calculation of water-use efficiency  
733 increases (Eq. A.18).

$$734 \quad ISW_y = ISW_{int} \cdot GVA_y \quad \text{Eq. (A.17)}$$

$$735 \quad IW_y = ISW_y \cdot TE^{y-y_{base}} \quad \text{Eq. (A.18)}$$

736 Where  $ISW$  is the yearly structural industrial withdrawal [ $m^3$ ],  $ISW_{int}$  the country specific industrial  
737 water intensity [ $m \text{ USD}_{equivalent}^{-1}$ ],  $IW$  the yearly industrial withdrawal [ $m^3$ ],  $GVA$  the yearly gross value  
738 added by industry [ $\text{USD}_{equivalent}$ ],  $y$  the year index,  $y_{base}$  the base year (taken to be the year when the  
739 industrial water intensity is determined), and  $TE$  the technological efficiency rate [-].

740  $TE$  was set at 0.976 and 1 for OECD and non-OECD countries respectively before the year 1980, 0.976  
741 between the years 1980 and 2000 and 0.99 after the year 2000 based on Flörke et al. (2013). Industrial  
742 water intensities were estimated for the 246 United Nations countries based on the GVA and industrial  
743 water withdrawal data. In case insufficient data was available to calculate the industrial water intensities,  
744 either sub-regional (56 countries), regional (17 countries) or global (9 countries) intensities estimates  
745 were used.

#### 746 **6.4.55.4.5 Energy sector**

747 For each thermoelectric power plant the water intensity was combined with their generation to calculate  
748 the water demands (Eq. A.19). Actual generation is estimated by adjusting the installed generation  
749 capacity by 46 % for fossil, 72 % for nuclear, and 56 % for biomass power plants (based on EIA national  
750 annual generation data (EIA, 2013)(EIA, 2013))

$$751 \quad EW_y = EW_{int} \cdot G_y \quad \text{Eq. (A.19)}$$

Formatted: Font: Italic

752 Where  $EW$  is the yearly energy withdrawal [ $m^3$ ],  $EW_{int}$  the energy water intensity [ $m^3 MWh^{-1}$ ],  $G$  the  
753 yearly generation for each plant [MWh], and  $y$  the year index.

754 The energy water demands were subtracted from the industrial water demands at the location of each  
755 power plant. In cases where the grid cell industrial water demand was less than the energy water demand,  
756 national industrial water demands were lowered. In cases where even the national industrial water  
757 demands were less than the national energy water demand (3 countries), the energy water demands were  
758 lowered instead. Energy demands were lowered until 10 % of the national industrial water demand  
759 remains, to ensure some spatial coverage of industrial and energy water demands.

#### 760 **6.4.6.5.4.6 Livestock sector**

761 Livestock water demands were estimated by combining the livestock population with the water  
762 requirements for each livestock variety (Eq. A.20).

$$763 \quad LW_y = LW_{int} \cdot L \quad \text{Eq. (A.20)}$$

764 Where  $LW$  is the yearly livestock withdrawal [ $m^3$ ],  $LW_{int}$  the livestock water intensity [ $m^3 livestock^{-1}$ ],  
765  $L$  the livestock number for each variety [livestock].

Formatted: Font: Italic

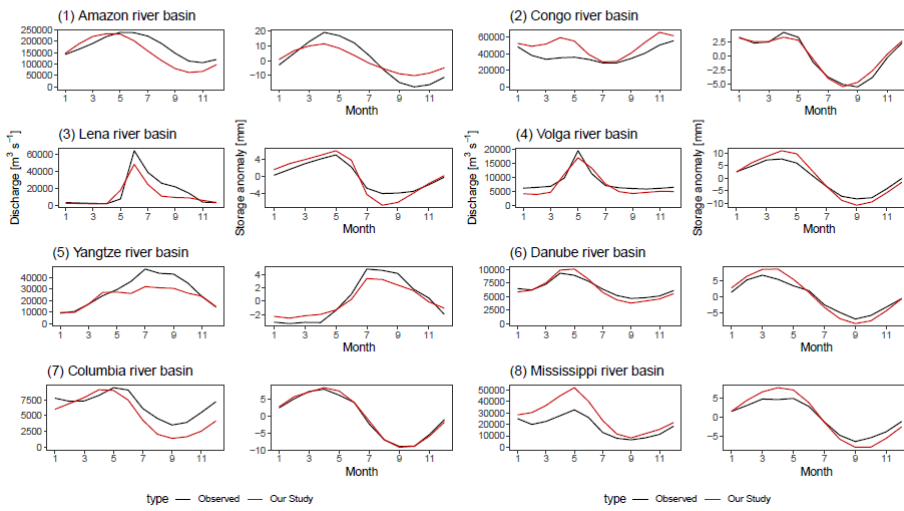
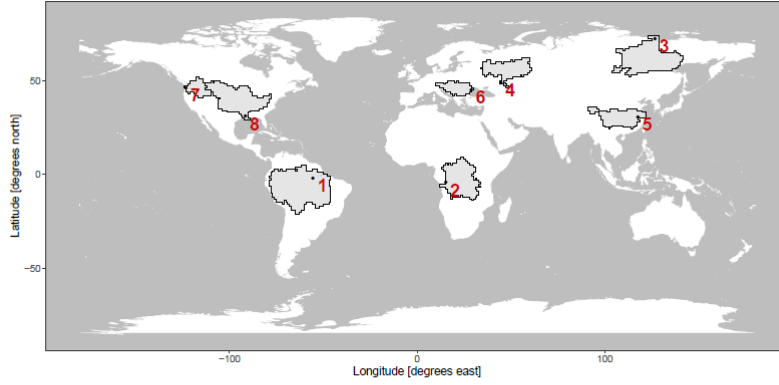
Formatted: Font: Italic

Formatted: Font: Italic

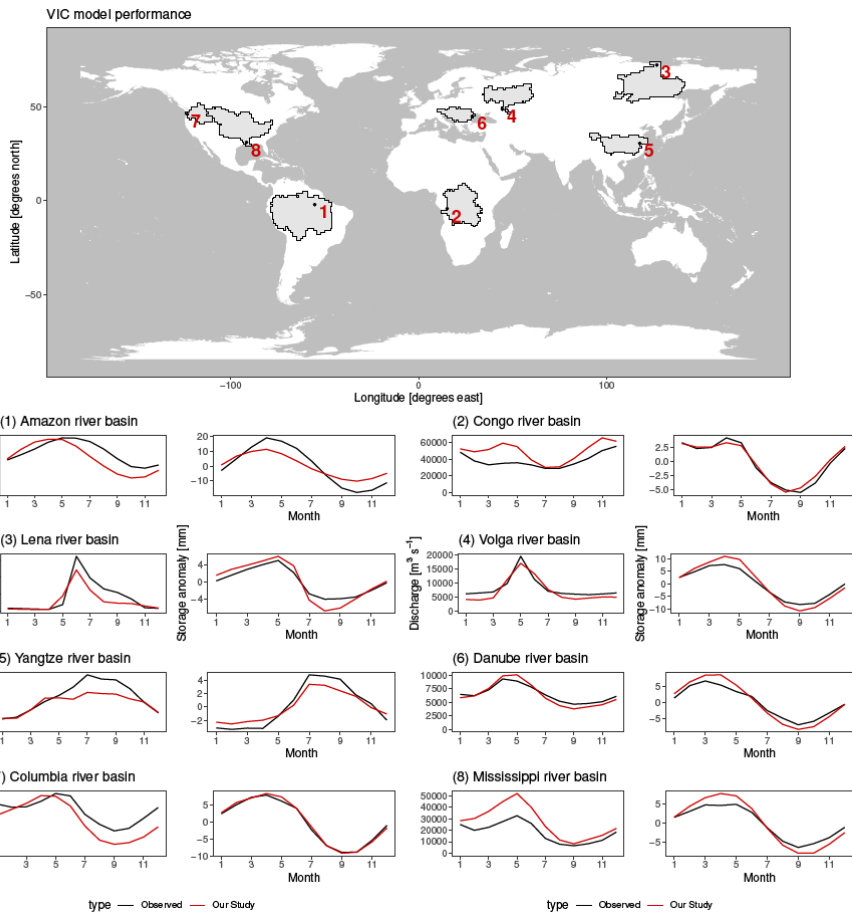
#### 766 **6.5.5 Appendix E: General performance**

767 VIC-WUR monthly discharge and monthly terrestrial total water storage anomalies were compared with  
768 observations from the GRDC dataset (~~GRDC, 2003~~)(GRDC, 2003) and GRACE satellite dataset  
769 (~~NASA, 2002~~)(NASA, 2002) for eight major river basins (not included in the main text; Fig. A1).  
770 Discharge stations were selected if the upstream area was larger than 10000 m<sup>2</sup>, matched the simulated  
771 upstream area at the station location,): Amazon, Congo, Lena, Volga, Yangtze, Danube, Columbia, and  
772 Mississippi river basins. A 300km gaussian filter has been applied to the total water storage simulation  
773 data (similar to Long et al. (2015)).

VIC model performance







775

776 **Figure A1: Comparison between simulated and GRDC and GRACE observed discharge and terrestrial total water**  
 777 **storage anomalies. Figures indicate multi-year averages of human-impacted simulations (red) and observations (black).**

778 **6 Code availability**

779 All code for the VIC-WUR model is freely available at [github.com/wur-wsg/VIC](https://github.com/wur-wsg/VIC) (tag VIC-WUR.2.1.0;  
 780 DOI 10.5281/zenodo.3934325) under the GNU General Public License, version 2 (GPL-2.0). VIC-  
 781 WUR documentation can be found at [vicwur.readthedocs.io](http://vicwur.readthedocs.io). The original VIC model is freely available  
 782 at [github.com/UW-Hydro/VIC](https://github.com/UW-Hydro/VIC) (tag VIC.5.0.1; DOI 10.5281/zenodo.267178) under the GNU General  
 783 Public License, version 2 (GPL-2.0). VIC documentation can be found at [vic.readthedocs.io](http://vic.readthedocs.io).  
 784 Documentation and scripts concerning input data used in our study is freely available at

785 [github.com/bramdr/VIC\\_support](https://github.com/bramdr/VIC_support) (tag VIC-WUR.2.1.0; DOI 10.5281/zenodo.3934363) under the GNU  
786 [General Public License, version 3 \(GPL-3.0\)](https://www.gnu.org/licenses/gpl-3.0/).

## 787 **7 Author contribution**

788 Bram Droppers and Wietse H.P. Franssen developed and tested the model additions introduced in VIC-  
789 WUR. Bram Droppers generated and analysed the results. Michelle T.H. van Vliet, Bart Nijssen and  
790 Fulco Ludwig provided overall oversight and guidance. Bram Droppers prepared the manuscript with  
791 contributions from all co-authors.

## 792 **8 Competing interests**

793 The authors declare that they have no conflict of interest.

## 794 **9 Acknowledgements**

795 We would like to thank Rik Leemans for his guidance and detailed comments. We would like to thank  
796 the Wageningen Institute for Environment and Climate Research (WIMEK) for providing funding for  
797 our research.

## 798 **10 References**

- 799 Abdulla, F. A., Lettenmaier, D. P., Wood, E. F., and Smith, J. A.: Application of a macroscale hydrologic  
800 model to estimate the water balance of the Arkansas Red River basin, *J Geophys Res-Atmos*,  
801 101, 7449-7459, 10.1029/95jd02416, 1996.
- 802 Alcamo, J., Döll, P., Kaspar, F., and Siebert, S.: Global change and global scenarios of water use and  
803 availability: an application of WaterGAP1.0, Center for environmental systems research,  
804 University of Kassel, Kassel, Germany, 96, 1997.
- 805 Alcamo, J., Döll, P., Henrichs, T., Kaspar, F., Lehner, B., Rosch, T., and Siebert, S.: Development and  
806 testing of the WaterGAP 2 global model of water use and availability, *Hydrolog Sci J*, 48, 317-  
807 337, 10.1623/hysj.48.3.317.45290, 2003.
- 808 Allen, R. G., Pereira, L. S., Raes, D., and Smith, M.: Crop Evapotranspiration - Guidelines for  
809 computing crop water requirements, Food and Agricultural Organisation, Rome, Italy, 326,  
810 1998.

811 Andreadis, K. M., Storck, P., and Lettenmaier, D. P.: Modeling snow accumulation and ablation  
812 processes in forested environments, *Water Resour Res*, 45, 10.1029/2008wr007042, 2009.

813 Babel, M. S., Das Gupta, A., and Pradhan, P.: A multivariate econometric approach for domestic water  
814 demand modeling: An application to Kathmandu, Nepal, *Water Resour Manag*, 21, 573-589,  
815 10.1007/s11269-006-9030-6, 2007.

816 Bazilian, M., Rogner, H., Howells, M., Hermann, S., Arent, D., Gielen, D., Steduto, P., Mueller, A.,  
817 Komor, P., Tol, R. S. J., and Yumkella, K. K.: Considering the energy, water and food nexus:  
818 Towards an integrated modelling approach, *Energ Policy*, 39, 7896-7906,  
819 10.1016/j.enpol.2011.09.039, 2011.

820 Best, M. J., Pryor, M., Clark, D. B., Rooney, G. G., Essery, R. L. H., Menard, C. B., Edwards, J. M.,  
821 Hendry, M. A., Porson, A., Gedney, N., Mercado, L. M., Sitch, S., Blyth, E., Boucher, O., Cox,  
822 P. M., Grimmond, C. S. B., and Harding, R. J.: The Joint UK Land Environment Simulator  
823 (JULES), model description - Part 1: Energy and water fluxes, *Geosci Model Dev*, 4, 677-699,  
824 10.5194/gmd-4-677-2011, 2011.

825 Biemans, H., Haddeland, I., Kabat, P., Ludwig, F., Hutjes, R. W. A., Heinke, J., von Bloh, W., and  
826 Gerten, D.: Impact of reservoirs on river discharge and irrigation water supply during the 20th  
827 century, *Water Resour Res*, 47, 10.1029/2009wr008929, 2011.

828 Bijl, D. L., Bogaart, P. W., Dekker, S. C., and van Vuuren, D. P.: Unpacking the nexus: Different spatial  
829 scales for water, food and energy, *Global Environ Chang*, 48, 22-31,  
830 10.1016/j.gloenvcha.2017.11.005, 2018.

831 Bolt, J., Inklaar, R., de Jong, H., and van Zanden, J. L.: Rebasings 'Maddison': New income comparisons  
832 and the shape of long-run economic developments, University of Groningen, Groningen, the  
833 Netherlands, 69, 2018.

834 Bondeau, A., Smith, P. C., Zaehle, S., Schaphoff, S., Lucht, W., Cramer, W., Gerten, D., Lotze-Campen,  
835 H., Muller, C., Reichstein, M., and Smith, B.: Modelling the role of agriculture for the 20th  
836 century global terrestrial carbon balance, *Global Change Biol*, 13, 679-706, 10.1111/j.1365-  
837 2486.2006.01305.x, 2007.

838 Bowling, L. C., Pomeroy, J. W., and Lettenmaier, D. P.: Parameterization of blowing-snow sublimation  
839 in a macroscale hydrology model, *J Hydrometeorol*, 5, 745-762, 10.1175/1525-  
840 7541(2004)005<0745:Pobsia>2.0.Co;2, 2004.

841 Brooks, R. H., and Corey, A. T.: Hydraulic properties of porous media, Colorado state university, Fort  
842 Collins, Colorado, 27, 1964.

843 Brouwer, C., Prins, K., and Heibloem, M.: Irrigation water management: Irrigation scheduling, Food  
844 and Agricultural Organisation, Rome, Italy, 66, 1989.

845 Calder, I. R.: Hydrologic effects of land use change, in: Handbook of hydrology, edited by: Maidment,  
846 D. R., McGraw-Hill, New York, 13, 1993.

847 Carpenter, S. R., Stanley, E. H., and Vander Zanden, M. J.: State of the World's Freshwater Ecosystems:  
848 Physical, Chemical, and Biological Changes, *Annu Rev Env Resour*, 36, 75-99,  
849 10.1146/annurev-environ-021810-094524, 2011.

850 Carter, A. J., and Scholes, R. J.: Generating a global database of soil properties, IGBP Data and  
851 Information Services, Potsdam, Germany, 10, 1999.

852 Chateau, J., Dellink, R., and Lanzi, E.: An overview of the OECD ENV-linkages model, *Organisation*  
853 *for economic co-operation and development*, 43, 2014.

854 Chegwiddden, O. S., Nijssen, B., Rupp, D. E., Arnold, J. R., Clark, M. P., Hamman, J. J., Kao, S.-C.,  
855 Mao, Y., Mizukami, N., Mote, P. W., Pan, M., Pytlak, E., and Xiao, M.: How Do Modeling  
856 Decisions Affect the Spread Among Hydrologic Climate Change Projections? Exploring a Large  
857 Ensemble of Simulations Across a Diversity of Hydroclimates, *Earth's Future*, 7, 623-637,  
858 10.1029/2018ef001047, 2019.

859 Cherkauer, K. A., and Lettenmaier, D. P.: Hydrologic effects of frozen soils in the upper Mississippi  
860 River basin, *J Geophys Res-Atmos*, 104, 19599-19610, 10.1029/1999jd900337, 1999.

861 Cherkauer, K. A., and Lettenmaier, D. P.: Simulation of spatial variability in snow and frozen soil, *J*  
862 *Geophys Res-Atmos*, 108, 10.1029/2003jd003575, 2003.

863 Connor, R.: Water for a sustainable world, United Nations Educational, Scientific and Cultural  
864 Organisation, Paris, France, 139, 2015.

865 Cosby, B. J., Hornberger, G. M., Clapp, R. B., and Ginn, T. R.: A Statistical Exploration of the  
866 Relationships of Soil-Moisture Characteristics to the Physical-Properties of Soils, *Water Resour*  
867 *Res*, 20, 682-690, 10.1029/WR020i006p00682, 1984.

868 de Graaf, I. E. M., van Beek, R. L. P. H., Gleeson, T., Moosdorf, N., Schmitz, O., Sutanudjaja, E. H.,  
869 and Bierkens, M. F. P.: A global-scale two-layer transient groundwater model: Development  
870 and application to groundwater depletion, *Adv Water Resour*, 102, 53-67,  
871 10.1016/j.advwatres.2017.01.011, 2017.

872 Deardorff, J. W.: Efficient Prediction of Ground Surface-Temperature and Moisture, with Inclusion of  
873 a Layer of Vegetation, *J Geophys Res-Oceans*, 83, 1889-1903, 10.1029/JC083iC04p01889,  
874 1978.

875 Döll, P., Fiedler, K., and Zhang, J.: Global-scale analysis of river flow alterations due to water  
876 withdrawals and reservoirs, *Hydrol Earth Syst Sc*, 13, 2413-2432, 2009.

877 Döll, P., Hoffmann-Dobrev, H., Portmann, F. T., Siebert, S., Eicker, A., Rodell, M., Strassberg, G., and  
878 Scanlon, B. R.: Impact of water withdrawals from groundwater and surface water on continental  
879 water storage variations, *J Geodyn*, 59-60, 143-156, 10.1016/j.jog.2011.05.001, 2012.

880 Döll, P., Müller Schmied, H., Schuh, C., Portmann, F. T., and Eicker, A.: Global-scale assessment of  
881 groundwater depletion and related groundwater abstractions: Combining hydrological modeling

882 with information from well observations and GRACE satellites, *Water Resour Res*, 50, 5698-  
883 5720, 10.1002/2014wr015595, 2014.

884 Döll, P., Douville, H., Guntner, A., Muller Schmied, H., and Wada, Y.: Modelling Freshwater Resources  
885 at the Global Scale: Challenges and Prospects, *Surv Geophys*, 37, 195-221, 10.1007/s10712-  
886 015-9343-1, 2016.

887 Ducoudre, N. I., Laval, K., and Perrier, A.: Sechiba, a New Set of Parameterizations of the Hydrologic  
888 Exchanges at the Land Atmosphere Interface within the Lmd Atmospheric General-Circulation  
889 Model, *J Climate*, 6, 248-273, 10.1175/1520-0442(1993)006<0248:Sansop>2.0.Co;2, 1993.

890 [EC: EUROSTAT, European Commission, 2019.](#)

891 [EIA: EIA, U.S. Energy Information Administration, 2013.](#)

892 Famiglietti, J. S.: The global groundwater crisis, *Nat Clim Change*, 4, 945-948, 10.1038/nclimate2425,  
893 2014.

894 [FAO: AQUASTAT, Food and agricultural organisation, 2016.](#)

895 Feenstra, R. C., Inklaar, R., and Timmer, M. P.: The Next Generation of the Penn World Table, *Am*  
896 *Econ Rev*, 105, 3150-3182, 10.1257/aer.20130954, 2015.

897 Flörke, M., and Alcamo, J.: European outlook on water use, Centre for environmental systems research,  
898 Kassel, 86, 2004.

899 Flörke, M., Kynast, E., Barlund, I., Eisner, S., Wimmer, F., and Alcamo, J.: Domestic and industrial  
900 water uses of the past 60 years as a mirror of socio-economic development: A global simulation  
901 study, *Global Environ Chang*, 23, 144-156, 10.1016/j.gloenvcha.2012.10.018, 2013.

902 Franchini, M., and Pacciani, M.: Comparative-Analysis of Several Conceptual Rainfall Runoff Models,  
903 *J Hydrol*, 122, 161-219, 10.1016/0022-1694(91)90178-K, 1991.

904 Frenken, K., and Gillet, V.: Irrigation water requirement and water withdrawal by country, Food and  
905 agricultural organisation, Rome, Italy, 264, 2012.

906 Gerten, D., Hoff, H., Rockstrom, J., Jagermeyr, J., Kummer, M., and Pastor, A. V.: Towards a revised  
907 planetary boundary for consumptive freshwater use: role of environmental flow requirements,  
908 *Curr Opin Env Sust*, 5, 551-558, 10.1016/j.cosust.2013.11.001, 2013.

909 Gilbert, M., Nicolas, G., Cinardi, G., Van Boeckel, T. P., Vanwambeke, S. O., Wint, G. R. W., and  
910 Robinson, T. P.: Global distribution data for cattle, buffaloes, horses, sheep, goats, pigs, chickens  
911 and ducks in 2010, *Sci Data*, 5, 10.1038/sdata.2018.227, 2018.

912 Gleeson, T., and Richter, B.: How much groundwater can we pump and protect environmental flows  
913 through time? Presumptive standards for conjunctive management of aquifers and rivers, *River*  
914 *Res Appl*, 34, 83-92, 10.1002/rra.3185, 2018.

915 Gleick, P. H., Cooley, H., Katz, D., Lee, E., Morrison, J., Meena, P., Samulon, A., and Wolff, G. H.:  
916 The world's water 2006-2007: The biennial report on freshwater resources, Island Press,  
917 Washington, 392 pp., 2013.

918 Goldewijk, K. K., Beusen, A., Doelman, J., and Stehfest, E.: Anthropogenic land use estimates for the  
919 Holocene - HYDE 3.2, *Earth Syst Sci Data*, 9, 927-953, 10.5194/essd-9-927-2017, 2017.

920 Goldstein, R., and Smith, W.: U.S. water consumption for power production - the next half century,  
921 Electric power research institute, California, United States, 57, 2002.

922 [GRDC: GRDC. The Global Runoff Data Centre, 2003.](#)

923 Grill, G., Lehner, B., Thieme, M., Geenen, B., Tickner, D., Antonelli, F., Babu, S., Borrelli, P., Cheng,  
924 L., Crochetiere, H., Macedo, H. E., Filgueiras, R., Goichot, M., Higgins, J., Hogan, Z., Lip, B.,  
925 McClain, M. E., Meng, J., Mulligan, M., Nilsson, C., Olden, J. D., Opperman, J. J., Petry, P.,  
926 Liermann, C. R., Saenz, L., Salinas-Rodriguez, S., Schelle, P., Schmitt, R. J. P., Snider, J., Tan,  
927 F., Tockner, K., Valdujo, P. H., van Soesbergen, A., and Zarfl, C.: Mapping the world's free-  
928 flowing rivers, *Nature*, 569, 215-+, 10.1038/s41586-019-1111-9, 2019.

929 Grobicki, A., Huidobro, P., Galloni, S., Asano, T., and Delgau, K. F.: Water, a shared responsibility  
930 (chapter 8), United Nations Educational, Scientific and Cultural Organisation, Paris, France,  
931 601, 2005.

932 Haddeland, I., Lettenmaier, D. P., and Skaugen, T.: Effects of irrigation on the water and energy balances  
933 of the Colorado and Mekong river basins, *J Hydrol*, 324, 210-223,  
934 10.1016/j.jhydrol.2005.09.028, 2006a.

935 Haddeland, I., Skaugen, T., and Lettenmaier, D. P.: Anthropogenic impacts on continental surface water  
936 fluxes, *Geophys Res Lett*, 33, 10.1029/2006gl026047, 2006b.

937 Hagemann, S., and Gates, L. D.: Validation of the hydrological cycle of ECMWF and NCEP reanalyses  
938 using the MPI hydrological discharge model, *J Geophys Res-Atmos*, 106, 1503-1510,  
939 10.1029/2000jd900568, 2001.

940 Hamlet, A. F., and Lettenmaier, D. P.: Effects of climate change on hydrology and water resources in  
941 the Columbia River basin, *J Am Water Resour As*, 35, 1597-1623, DOI 10.1111/j.1752-  
942 1688.1999.tb04240.x, 1999.

943 Hamman, J., Nijssen, B., Brunke, M., Cassano, J., Craig, A., DuVivier, A., Hughes, M., Lettenmaier,  
944 D. P., Maslowski, W., Osinski, R., Roberts, A., and Zeng, X. B.: Land Surface Climate in the  
945 Regional Arctic System Model, *J Climate*, 29, 6543-6562, 10.1175/Jcli-D-15-0415.1, 2016.

946 Hamman, J., Nijssen, B., Roberts, A., Craig, A., Maslowski, W., and Osinski, R.: The coastal streamflow  
947 flux in the Regional Arctic System Model, *J Geophys Res-Oceans*, 122, 1683-1701,  
948 10.1002/2016jc012323, 2017.

949 Hamman, J. J., Nijssen, B., Bohn, T. J., Gergel, D. R., and Mao, Y. X.: The Variable Infiltration Capacity  
950 model version 5 (VIC-5): infrastructure improvements for new applications and reproducibility,  
951 *Geosci Model Dev*, 11, 3481-3496, 10.5194/gmd-11-3481-2018, 2018.

952 Hanasaki, N., Kanae, S., and Oki, T.: A reservoir operation scheme for global river routing models, *J*  
953 *Hydrol*, 327, 22-41, 10.1016/j.jhydrol.2005.11.011, 2006.

954 Hanasaki, N., Kanae, S., Oki, T., Masuda, K., Motoya, K., Shirakawa, N., Shen, Y., and Tanaka, K.: An  
955 integrated model for the assessment of global water resources Part 2: Applications and  
956 assessments, *Hydrol Earth Syst Sc*, 12, 1027-1037, 10.5194/hess-12-1027-2008, 2008a.

957 Hanasaki, N., Kanae, S., Oki, T., Masuda, K., Motoya, K., Shirakawa, N., Shen, Y., and Tanaka, K.: An  
958 integrated model for the assessment of global water resources Part 1: Model description and  
959 input meteorological forcing, *Hydrol Earth Syst Sc*, 12, 1007-1025, 10.5194/hess-12-1007-  
960 2008, 2008b.

961 Hanasaki, N., Fujimori, S., Yamamoto, T., Yoshikawa, S., Masaki, Y., Hijioka, Y., Kainuma, M.,  
962 Kanamori, Y., Masui, T., and Takahashi, K.: A global water scarcity assessment under Shared  
963 Socio-economic Pathways—Part 1: Water use, *Hydrol Earth Syst Sc*, 17, 2375-2391, 2013.

964 Hanasaki, N., Yoshikawa, S., Pokhrel, Y., and Kanae, S.: A global hydrological simulation to specify  
965 the sources of water used by humans, *Hydrol Earth Syst Sc*, 22, 789-817, 10.5194/hess-22-789-  
966 2018, 2018.

967 Hansen, M. C., Defries, R. S., Townshend, J. R. G., and Sohlberg, R.: Global land cover classification  
968 at 1km spatial resolution using a classification tree approach, *Int J Remote Sens*, 21, 1331-1364,  
969 Doi 10.1080/014311600210209, 2000.

970 Harding, R., Best, M., Blyth, E., Hagemann, S., Kabat, P., Tallaksen, L. M., Warnaars, T., Wiberg, D.,  
971 Weedon, G. P., Lanen, H. v., Ludwig, F., and Haddeland, I.: WATCH: Current Knowledge of  
972 the Terrestrial Global Water Cycle, *J Hydrometeorol*, 12, 1149-1156, 10.1175/jhm-d-11-024.1,  
973 2011.

974 Hejazi, M., Edmonds, J., Clarke, L., Kyle, P., Davies, E., Chaturvedi, V., Wise, M., Patel, P., Eom, J.,  
975 Calvin, K., Moss, R., and Kim, S.: Long-term global water projections using six socioeconomic  
976 scenarios in an integrated assessment modeling framework, *Technol Forecast Soc*, 81, 205-226,  
977 10.1016/j.techfore.2013.05.006, 2014.

978 Huang, Z., Hejazi, M., Li, X., Tang, Q., Vernon, C., Leng, G., Liu, Y., Döll, P., Eisner, S., Gerten, D.,  
979 Hanasaki, N., and Wada, Y.: Reconstruction of global gridded monthly sectoral water  
980 withdrawals for 1971–2010 and analysis of their spatiotemporal patterns, *Hydrol. Earth Syst.  
981 Sci.*, 22, 2117-2133, 10.5194/hess-22-2117-2018, 2018.

982 Jägermeyr, J., Pastor, A., Biemans, H., and Gerten, D.: Reconciling irrigated food production with  
983 environmental flows for Sustainable Development Goals implementation, *Nature  
984 Communications*, 8, 15900, 10.1038/ncomms15900, 2017.

985 Kim, S. H., Hejazi, M., Liu, L., Calvin, K., Clarke, L., Edmonds, J., Kyle, P., Patel, P., Wise, M., and  
986 Davies, E.: Balancing global water availability and use at basin scale in an integrated assessment  
987 model, *Climatic Change*, 136, 217-231, 10.1007/s10584-016-1604-6, 2016.

988 Konikow, L. F.: Contribution of global groundwater depletion since 1900 to sea-level rise, *Geophys Res  
989 Lett*, 38, 10.1029/2011gl048604, 2011.

990 Krinner, G., Viovy, N., de Noblet-Duoudre, N., Ogee, J., Polcher, J., Friedlingstein, P., Ciais, P., Sitch,  
991 S., and Prentice, I. C.: A dynamic global vegetation model for studies of the coupled atmosphere-  
992 biosphere system, *Global Biogeochem Cy*, 19, 10.1029/2003gb002199, 2005.

993 Lehner, B., Liermann, C. R., Revenga, C., Vorosmarty, C., Fekete, B., Crouzet, P., Döll, P., Endejan,  
994 M., Frenken, K., Magome, J., Nilsson, C., Robertson, J. C., Rodel, R., Sindorf, N., and Wisser,  
995 D.: High-resolution mapping of the world's reservoirs and dams for sustainable river-flow  
996 management, *Front Ecol Environ*, 9, 494-502, 10.1890/100125, 2011.

997 Liang, X., Lettenmaier, D. P., Wood, E. F., and Burges, S. J.: A Simple Hydrologically Based Model of  
998 Land-Surface Water and Energy Fluxes for General-Circulation Models, *J Geophys Res-Atmos*,  
999 99, 14415-14428, 10.1029/94jd00483, 1994.

1000 Lohmann, D., Nolte-Holube, R., and Raschke, E.: A large-scale horizontal routing model to be coupled  
1001 to land surface parametrization schemes, *Tellus A*, 48, 708-721, 10.1034/j.1600-0870.1996.t01-  
1002 3-00009.x, 1996.

1003 Lohmann, D., Raschke, E., Nijssen, B., and Lettenmaier, D. P.: Regional scale hydrology: ~~II. Formulation~~  
1004 ~~II. Application~~ of the VIC-2L model ~~coupled to a routing model~~ the Weser River, Germany,  
1005 *Hydrolog Sci J*, 43, ~~131-141~~ 143-158,  
1006 10.1080/~~02626669809492107~~ 02626669809492108, 1998a.

1007 Lohmann, D., Raschke, E., Nijssen, B., and Lettenmaier, D. P.: Regional scale hydrology: ~~II. Application~~  
1008 ~~I. Formulation~~ of the VIC-2L model ~~coupled to the Weser River, Germany~~ a routing  
1009 model, *Hydrolog Sci J*, 43, ~~143-158~~ 131-141,  
1010 10.1080/~~02626669809492108~~ 02626669809492107, 1998b.

1011 Long, D., Yang, Y., Wada, Y., Hong, Y., Liang, W., Chen, Y., Yong, B., Hou, A., Wei, J., and Chen,  
1012 L.: Deriving scaling factors using a global hydrological model to restore GRACE total water  
1013 storage changes for China's Yangtze River Basin, *Remote Sens Environ*, 168, 177-193,  
1014 10.1016/j.rse.2015.07.003, 2015.

1015 Masaki, Y., Hanasaki, N., Takahashi, K., and Hijikata, Y.: Consequences of implementing a reservoir  
1016 operation algorithm in a global hydrological model under multiple meteorological forcing,  
1017 *Hydrological Sciences Journal*, 63, 1047-1061, 10.1080/02626667.2018.1473872, 2018.

1018 Mekonnen, M. M., and Hoekstra, A. Y.: Four billion people facing severe water scarcity, *Sci Adv*, 2,  
1019 10.1126/sciadv.1500323, 2016.

1020 Mo, K. C.: Model-Based Drought Indices over the United States, *J Hydrometeorol*, 9, 1212-1230,  
1021 10.1175/2008jhm1002.1, 2008.

1022 Myneni, R. B., Nemani, R. R., and Running, S. W.: Estimation of global leaf area index and absorbed  
1023 par using radiative transfer models, *Ieee T Geosci Remote*, 35, 1380-1393, 10.1109/36.649788,  
1024 1997.

1025 NASA: GRACE, National Aeronautics and Space Administration, 2002.



1026 Nazemi, A., and Wheater, H. S.: On inclusion of water resource management in Earth system models -  
1027 Part 2: Representation of water supply and allocation and opportunities for improved modeling,  
1028 Hydrol Earth Syst Sc, 19, 63-90, 10.5194/hess-19-63-2015, 2015a.

1029 Nazemi, A., and Wheater, H. S.: On inclusion of water resource management in Earth system models -  
1030 Part 1: Problem definition and representation of water demand, Hydrol Earth Syst Sc, 19, 33-61,  
1031 10.5194/hess-19-33-2015, 2015b.

1032 Nijssen, B., Lettenmaier, D. P., Liang, X., Wetzel, S. W., and Wood, E. F.: Streamflow simulation for  
1033 continental-scale river basins, Water Resour Res, 33, 711-724, 10.1029/96wr03517, 1997.

1034 Nijssen, B., O'Donnell, G. M., Hamlet, A. F., and Lettenmaier, D. P.: Hydrologic sensitivity of global  
1035 rivers to climate change, Climatic Change, 50, 143-175, 10.1023/A:1010616428763, 2001a.

1036 Nijssen, B., O'Donnell, G. M., Lettenmaier, D. P., Lohmann, D., and Wood, E. F.: Predicting the  
1037 discharge of global rivers, J Climate, 14, 3307-3323, 10.1175/1520-  
1038 0442(2001)014<3307:Ptdogr>2.0.Co;2, 2001b.

1039 Nijssen, B., Schnur, R., and Lettenmaier, D. P.: Global retrospective estimation of soil moisture using  
1040 the variable infiltration capacity land surface model, 1980-93, J Climate, 14, 1790-1808,  
1041 10.1175/1520-0442(2001)014<1790:Greosm>2.0.Co;2, 2001c.

1042 Nilsson, C., Reidy, C. A., Dynesius, M., and Revenga, C.: Fragmentation and flow regulation of the  
1043 world's large river systems, Science, 308, 405-408, 10.1126/science.1107887, 2005.

1044 Oki, T., Musiak, K., Matsuyama, H., and Masuda, K.: Global Atmospheric Water-Balance and Runoff  
1045 from Large River Basins, Hydrol Process, 9, 655-678, 10.1002/hyp.3360090513, 1995.

1046 Oki, T., and Kanae, S.: Global hydrological cycles and world water resources, Science, 313, 1068-1072,  
1047 10.1126/science.1128845, 2006.

1048 Pastor, A. V., Ludwig, F., Biemans, H., Hoff, H., and Kabat, P.: Accounting for environmental flow  
1049 requirements in global water assessments, Hydrol Earth Syst Sc, 18, 5041-5059, 10.5194/hess-  
1050 18-5041-2014, 2014.

1051 Pastor, A. V., Palazzo, A., Havlik, P., Biemans, H., Wada, Y., Obersteiner, M., Kabat, P., and Ludwig,  
1052 F.: The global nexus of food–trade–water sustaining environmental flows by 2050, Nature  
1053 Sustainability, 2, 499-507, 10.1038/s41893-019-0287-1, 2019.

1054 Poff, N. L., Richter, B. D., Arthington, A. H., Bunn, S. E., Naiman, R. J., Kendy, E., Acreman, M.,  
1055 Apse, C., Bledsoe, B. P., Freeman, M. C., Henriksen, J., Jacobson, R. B., Kennen, J. G., Merritt,  
1056 D. M., O'Keeffe, J. H., Olden, J. D., Rogers, K., Tharme, R. E., and Warner, A.: The ecological  
1057 limits of hydrologic alteration (ELOHA): a new framework for developing regional  
1058 environmental flow standards, Freshwater Biol, 55, 147-170, 10.1111/j.1365-  
1059 2427.2009.02204.x, 2010.

1060 Pokhrel, Y., Hanasaki, N., Koirala, S., Cho, J., Yeh, P. J.-F., Kim, H., Kanae, S., and Oki, T.:  
1061 Incorporating Anthropogenic Water Regulation Modules into a Land Surface Model, *J*  
1062 *Hydrometeorol*, 13, 255-269, 10.1175/jhm-d-11-013.1, 2012a.

1063 Pokhrel, Y., Hanasaki, N., Koirala, S., Cho, J., Yeh, P. J. F., Kim, H., Kanae, S., and Oki, T.:  
1064 Incorporating Anthropogenic Water Regulation Modules into a Land Surface Model, *J*  
1065 *Hydrometeorol*, 13, 255-269, 10.1175/Jhm-D-11-013.1, 2012b.

1066 Pokhrel, Y. N., Koirala, S., Yeh, P. J.-F., Hanasaki, N., Longuevergne, L., Kanae, S., and Oki, T.:  
1067 Incorporation of groundwater pumping in a global Land Surface Model with the representation  
1068 of human impacts, *Water Resour Res*, 51, 78-96, 10.1002/2014wr015602, 2015.

1069 Pokhrel, Y. N., Hanasaki, N., Wada, Y., and Kim, H.: Recent progresses in incorporating human land-  
1070 water management into global land surface models toward their integration into Earth system  
1071 models, *Wires Water*, 3, 548-574, 10.1002/wat2.1150, 2016.

1072 Portmann, F. T., Siebert, S., and Döll, P.: MIRCA2000-Global monthly irrigated and rainfed crop areas  
1073 around the year 2000: A new high-resolution data set for agricultural and hydrological modeling,  
1074 *Global Biogeochem Cy*, 24, 10.1029/2008gb003435, 2010.

1075 Postel, S. L., Daily, G. C., and Ehrlich, P. R.: Human appropriation of renewable fresh water, *Science*,  
1076 271, 785-788, 10.1126/science.271.5250.785, 1996.

1077 Reed, B., and Reed, B.: How much water is needed in emergencies, *Water, Engineering and*  
1078 *Development Centre*, Leicestershire, 2013.

1079 Richter, B. D., Davis, M. M., Apse, C., and Konrad, C.: A Presumptive Standard for Environmental  
1080 Flow Protection, *River Res Appl*, 28, 1312-1321, 10.1002/rra.1511, 2012.

1081 Rodell, M., Velicogna, I., and Famiglietti, J. S.: Satellite-based estimates of groundwater depletion in  
1082 India, *Nature*, 460, 999-U980, 10.1038/nature08238, 2009.

1083 Roman, M. O., Wang, Z. S., Sun, Q. S., Kalb, V., Miller, S. D., Molthan, A., Schultz, L., Bell, J., Stokes,  
1084 E. C., Pandey, B., Seto, K. C., Hall, D., Oda, T., Wolfe, R. E., Lin, G., Golpayegani, N.,  
1085 Devadiga, S., Davidson, C., Sarkar, S., Praderas, C., Schmaltz, J., Boller, R., Stevens, J.,  
1086 Gonzalez, O. M. R., Padilla, E., Alonso, J., Detres, Y., Armstrong, R., Miranda, I., Conte, Y.,  
1087 Marrero, N., MacManus, K., Esch, T., and Masuoka, E. J.: NASA's Black Marble nighttime  
1088 lights product suite, *Remote Sens Environ*, 210, 113-143, 10.1016/j.rse.2018.03.017, 2018.

1089 Rost, S., Gerten, D., Bondeau, A., Lucht, W., Rohwer, J., and Schaphoff, S.: Agricultural green and blue  
1090 water consumption and its influence on the global water system, *Water Resour Res*, 44,  
1091 10.1029/2007wr006331, 2008.

1092 Rougé, C., Reed, P. M., Grogan, D. S., Zuidema, S., Prusevich, A., Glidden, S., Lamontagne, J. R., and  
1093 Lammers, R. B.: Coordination and Control: Limits in Standard Representations of Multi-  
1094 Reservoir Operations in Hydrological Modeling, *Hydrol. Earth Syst. Sci. Discuss.*, 2019, 1-37,  
1095 10.5194/hess-2019-589, 2019.

1096 Sellers, P. J., Tucker, C. J., Collatz, G. J., Los, S. O., Justice, C. O., Dazlich, D. A., and Randall, D. A.:  
1097 A Global 1-Degrees-by-1-Degrees Ndvi Data Set for Climate Studies .2. The Generation of  
1098 Global Fields of Terrestrial Biophysical Parameters from the Ndvi, *Int J Remote Sens*, 15, 3519-  
1099 3545, 10.1080/01431169408954343, 1994.

1100 Shen, Y., Oki, T., Utsumi, N., Kanae, S., and Hanasaki, N.: Projection of future world water resources  
1101 under SRES scenarios: water withdrawal/Projection des ressources en eau mondiales futures  
1102 selon les scénarios du RSSE: prélèvement d'eau, *Hydrological sciences journal*, 53, 11-33,  
1103 [10.1080/02626667.2013.862338](https://doi.org/10.1080/02626667.2013.862338), 2008.

1104 Shiklomanov, I. A.: Appraisal and assessment of world water resources, *Water Int*, 25, 11-32, Doi  
1105 10.1080/02508060008686794, 2000.

1106 Shuttleworth, W. J.: Evaporation, in: *Handbook of hydrology*, edited by: Maidment, D. R., McGraw-  
1107 Hill, New York, 53, 1993.

1108 Smakhtin, V., Revenga, C., and Döll, P.: A pilot global assessment of environmental water requirements  
1109 and scarcity, *Water Int*, 29, 307-317, 10.1080/02508060408691785, 2004.

1110 Smith, M.: CROPWAT: A computer program for irrigation planning and ~~managemetn~~management,  
1111 [FAO irrigation and drainage paper](#), Food and Agricultural Organisation, Rome, Italy, 127, pp.,  
1112 1996.

1113 Steinfeld, H., Gerber, P., Wassenaar, T. D., Castel, V., Rosales, M., and De Haan, C.: *Livestock's long  
1114 shadow: environmental issues and options*, Food and Agricultural Organisation, Rome, Italy,  
1115 416 pp., 2006.

1116 Sutanudjaja, E. H., van Beek, R., Wanders, N., Wada, Y., Bosmans, J. H. C., Drost, N., van der Ent, R.  
1117 J., de Graaf, I. E. M., Hoch, J. M., de Jong, K., Karssenber, D., Lopez, P. L., Pessenteiner, S.,  
1118 Schmitz, O., Straatsma, M. W., Vannamete, E., Wisser, D., and Bierkens, M. F. P.: PCR-  
1119 GLOBWB 2: a 5 arcmin global hydrological and water resources model, *Geosci Model Dev*, 11,  
1120 2429-2453, 10.5194/gmd-11-2429-2018, 2018.

1121 Takata, K., Emori, S., and Watanabe, T.: Development of the minimal advanced treatments of surface  
1122 interaction and runoff, *Global Planet Change*, 38, 209-222, 10.1016/S0921-8181(03)00030-4,  
1123 2003.

1124 Tessler, Z. D., Vorosmarty, C. J., Grossberg, M., Gladkova, I., Aizenman, H., Syvitski, J. P. M., and  
1125 Foufoula-Georgiou, E.: Profiling risk and sustainability in coastal deltas of the world, *Science*,  
1126 349, 638-643, 10.1126/science.aab3574, 2015.

1127 Turner, S. W. D., Hejazi, M., Yonkofski, C., Kim, S. H., and Kyle, P.: Influence of Groundwater  
1128 Extraction Costs and Resource Depletion Limits on Simulated Global Nonrenewable Water  
1129 Withdrawals Over the Twenty-First Century, *Earth's Future*, 7, 123-135,  
1130 10.1029/2018ef001105, 2019.

Formatted: Dutch (Netherlands)

1131 ~~Van~~ van Beek, L. P. H., and Bierkens, M. F. P.: The global hydrological model PCR-GLOBWB:  
1132 conceptualization, parameterization and verification, Departement of physical geography,  
1133 Utrecht university, Utrecht, The Netherlands, 53, ~~2008~~2009.

1134 van Vliet, M. T. H., Wiberg, D., Leduc, S., and Riahi, K.: Power-generation system vulnerability and  
1135 adaptation to changes in climate and water resources, *Nat Clim Change*, 6, 375-+,  
1136 10.1038/Nclimate2903, 2016.

1137 Vassolo, S., and Döll, P.: Global-scale gridded estimates of thermoelectric power and manufacturing  
1138 water use, *Water Resour Res*, 41, 10.1029/2004wr003360, 2005.

1139 Voisin, N., Li, H., Ward, D., Huang, M., Wigmosta, M., and Leung, L.: On an improved sub-regional  
1140 water resources management representation for integration into earth system models, *Hydrology  
1141 & Earth System Sciences*, 17, [10.5194/hess-17-3605-2013](https://doi.org/10.5194/hess-17-3605-2013), 2013a.

1142 Voisin, N., Li, H., Ward, D., Huang, M., Wigmosta, M., and Leung, L. R.: On an improved sub-regional  
1143 water resources management representation for integration into earth system models, *Hydrol  
1144 Earth Syst Sc*, 17, 3605-3622, [10.5194/hess-17-3605-2013](https://doi.org/10.5194/hess-17-3605-2013), 2013b.

1145 Voisin, N., Hejazi, M. I., Leung, L. R., Liu, L., Huang, M. Y., Li, H. Y., and Tesfa, T.: Effects of  
1146 spatially distributed sectoral water management on the redistribution of water resources in an  
1147 integrated water model, *Water Resour Res*, 53, 4253-4270, [10.1002/2016wr019767](https://doi.org/10.1002/2016wr019767), 2017.

1148 Voisin, N., Kintner-Meyer, M., Wu, D., Skaggs, R., Fu, T., Zhou, T., Nguyen, T., and Kraucunas, I.:  
1149 OPPORTUNITIES FOR JOINT WATER-ENERGY MANAGEMENT Sensitivity of the 2010  
1150 Western US Electricity Grid Operations to Climate Oscillations, *B Am Meteorol Soc*, 99, 299-  
1151 312, [10.1175/Bams-D-16-0253.1](https://doi.org/10.1175/Bams-D-16-0253.1), 2018.

1152 Vorosmarty, C. J., McIntyre, P. B., Gessner, M. O., Dudgeon, D., Prusevich, A., Green, P., Glidden, S.,  
1153 Bunn, S. E., Sullivan, C. A., Liermann, C. R., and Davies, P. M.: Global threats to human water  
1154 security and river biodiversity, *Nature*, 467, 555-561, [10.1038/nature09440](https://doi.org/10.1038/nature09440), 2010.

1155 Voß, F., and Flörke, M.: Spatially explicit estimates of past and present manufacturing and energy water  
1156 use, *Center for environmental systems research, Kassel*, 17, 2010.

1157 Wada, Y., van Beek, L. P. H., and Bierkens, M. F. P.: Modelling global water stress of the recent past:  
1158 on the relative importance of trends in water demand and climate variability, *Hydrol Earth Syst  
1159 Sc*, 15, 3785-3808, [10.5194/hess-15-3785-2011](https://doi.org/10.5194/hess-15-3785-2011), 2011a.

1160 Wada, Y., van Beek, L. P. H., Viviroli, D., Durr, H. H., Weingartner, R., and Bierkens, M. F. P.: Global  
1161 monthly water stress: 2. Water demand and severity of water stress, *Water Resour Res*, 47,  
1162 [10.1029/2010wr009792](https://doi.org/10.1029/2010wr009792), 2011b.

1163 Wada, Y., and Bierkens, M. F. P.: Sustainability of global water use: past reconstruction and future  
1164 projections, *Environ Res Lett*, 9, 104003, [10.1088/1748-9326/9/10/104003](https://doi.org/10.1088/1748-9326/9/10/104003), 2014.

1165 Wada, Y., Wisser, D., and Bierkens, M. F. P.: Global modeling of withdrawal, allocation and  
1166 consumptive use of surface water and groundwater resources, *Earth Syst Dynam*, 5, 15-40,  
1167 10.5194/esd-5-15-2014, 2014.

1168 Weedon, G. P., Balsamo, G., Bellouin, N., Gomes, S., Best, M. J., and Viterbo, P.: The WFDEI  
1169 meteorological forcing data set: WATCH Forcing Data methodology applied to ERA-Interim  
1170 reanalysis data, *Water Resour Res*, 50, 7505-7514, 10.1002/2014wr015638, 2014.

1171 Wisser, D., Fekete, B. M., Vorosmarty, C. J., and Schumann, A. H.: Reconstructing 20th century global  
1172 hydrography: a contribution to the Global Terrestrial Network- Hydrology (GTN-H), *Hydrol*  
1173 *Earth Syst Sc*, 14, 1-24, 10.5194/hess-14-1-2010, 2010a.

1174 Wisser, D., Fekete, B. M., Vörösmarty, C. J., and Schumann, A. H.: Reconstructing 20th century global  
1175 hydrography: a contribution to the Global Terrestrial Network- Hydrology (GTN-H), *Hydrol.*  
1176 *Earth Syst. Sci.*, 14, 1-24, 10.5194/hess-14-1-2010, 2010b.

1177 Wood, A. W., and Lettenmaier, D. P.: A test bed for new seasonal hydrologic forecasting approaches in  
1178 the western United States, *B Am Meteorol Soc*, 87, 1699-+, 10.1175/Bams-87-12-1699, 2006.

1179 [World bank: World bank development indicators, World bank, 2010.](#)

1180 Yassin, F., Razavi, S., Elshamy, M., Davison, B., Sapriza-Azuri, G., and Wheater, H.: Representation  
1181 and improved parameterization of reservoir operation in hydrological and land-surface models,  
1182 *Hydrol. Earth Syst. Sci.*, 23, 3735-3764, 10.5194/hess-23-3735-2019, 2019.

1183 Zhao, G., Gao, H. L., Naz, B. S., Kao, S. C., and Voisin, N.: Integrating a reservoir regulation scheme  
1184 into a spatially distributed hydrological model, *Adv Water Resour*, 98, 16-31,  
1185 10.1016/j.advwatres.2016.10.014, 2016.

1186 Zhou, T., Haddeland, I., Nijssen, B., and Lettenmaier, D. P.: Human induced changes in the global water  
1187 cycle, *AGU Geophysical Monograph Series*, ~~Submitted~~[10.1002/9781118971772.ch4](#), 2015.

1188 Zhou, T., Nijssen, B., Gao, H. L., and Lettenmaier, D. P.: The Contribution of Reservoirs to Global  
1189 Land Surface Water Storage Variations, *J Hydrometeorol*, 17, 309-325, 10.1175/Jhm-D-15-  
1190 0002.1, 2016.

1191 Zhou, T., Voisin, N., Leng, G. Y., Huang, M. Y., and Kraucunas, I.: Sensitivity of Regulated Flow  
1192 Regimes to Climate Change in the Western United States, *J Hydrometeorol*, 19, 499-515,  
1193 10.1175/Jhm-D-17-0095.1, 2018.

1194 Zhu, C. M., Leung, L. R., Gochis, D., Qian, Y., and Lettenmaier, D. P.: Evaluating the Influence of  
1195 Antecedent Soil Moisture on Variability of the North American Monsoon Precipitation in the  
1196 Coupled MM5/VIC Modeling System, *J Adv Model Earth Sy*, 1, 10.3894/James.2009.1.13,  
1197 2009.

1198